Quaternary Science Reviews 143 (2016) 37–50

Contents lists available at ScienceDirect

Quaternary Science Reviews

journal homepage: www.elsevier.com/locate/quascirev

Dating the onset of LGM ice surface lowering in the High Alps

Christian Wirsig [a], Jerzy Zasadni [b, *], Marcus Christl [a], Naki Akçar [c], Susan Ivy-Ochs [a]

[a] Laboratory of Ion Beam Physics, ETH Zürich, Otto-Stern-Weg 5, 8093 Zürich, Switzerland
[b] Faculty of Geology, Geophysics and Environmental Protection, AGH University of Science and Technology, al. A. Mickiewicza 30, 30-059 Kraków, Poland
[c] Institute of Geological Sciences, University of Bern, Baltzerstrasse 1+3, 3012 Bern, Switzerland

ARTICLE INFO

Article history:
Received 17 December 2015
Received in revised form
30 April 2016
Accepted 4 May 2016
Available online 18 May 2016

Keywords:
^{10}Be
Deglaciation
Zillertal
Mont Blanc

ABSTRACT

The general chronological outline of the Last Glacial Maximum (LGM) in the Alps is well known after more than two centuries of ice age research in Europe. Current studies focus on resolving the details of the deglaciation process after the LGM. Particularly few data in this context are available from the High Alps. Here we report chronological constraints on the onset of deglaciation in two different study areas from the Western and Eastern Alps: the Mont Blanc (Italy) and Zillertal Alps (Austria). We sampled 32 bedrock and boulder surfaces from high elevation ridges beneath the glacial trimline. The oldest ^{10}Be exposure ages of ~18.5 ka correspond to the initiation of lowering of the LGM ice surface. Identical ages from both study areas suggest synchronous decay of the LGM glaciers in the accumulation zones of the Western and Eastern Alps. Thus, the High Alpine ice surface lowered roughly synchronously to the downwasting of the glacier tongues in the forelands that was completed 19–18 ka. In both study areas, ages of numerous samples that are consistently 2–3 ka younger than 18.5 ka suggest the persistance of remnant ice patches at high elevations in the Lateglacial accumulation zones approximately until the Bølling-Allerød interstadial.

1. Introduction

The Alps are the largest mountain range in Central Europe. They stretch in a wide arc from southern France in the west to Slovenia in the east over a distance of approximately 1200 km. The Alpine divide (Fig. 1A) at its center is often more than 3000 m high. It controls precipitation patterns and thereby sketches the outline of climate zones in neighboring regions: maritime climate to the west, Mediterranean climate to the south and more continental climate to the northeast (Veit, 2002, and references therein). Today only the highest areas above ~2500–3000 m are occupied by glaciers and permafrost (Hoelzle, 1996; Evans, 2006). In contrast, during the Last Glacial Maximum (LGM – 26.5–19 ka; Clark et al., 2009) the Alps were almost completely covered by ice (Fig. 1A). The accumulation zones within the High Alps sustained an extensive network of transections glaciers that filled the main valleys (Penck and Brückner, 1901/1909; Jäckli, 1962; van Husen, 1987). Whereas a few dispersive centers of ice accumulation dominated the Central Swiss Alps (Florineth and Schlüchter, 1998; Kelly et al., 2004; Bini et al., 2009), glaciers in the Eastern Alps and southern side of the Western Alps were more strongly controlled by topography (Mayr and Heuberger, 1968; van Husen, 1987). Large ice masses in the main valleys fed outlet piedmont lobes which extended into the northern and southern Alpine forelands (Penck and Brückner, 1901/1909).

The maximum dimension of ice cover in the High Alps is well recorded in the glacial trimline (Ballantyne, 1997) that is visible in the topography as the boundary between an ice-moulded downslope area and a frost-shattered upslope zone (Florineth and Schlüchter, 1998; Kelly et al., 2004). In large-scale morphology, the trimline is commonly discernible as a truncation of valley-side spurs showing a more or less sharp transition (30–100 m) between the frost-weathered arête zone above and the gentle ice-moulded ridges below (Florineth, 1998; Hippe et al., 2014; Wirsig et al., 2016). It is generally assumed in the Alps that the trimline represents the maximum elevation of the active LGM ice surface (subaerial/subglacial boundary) (Florineth and Schlüchter, 1998; Kelly et al., 2004; Cossart et al., 2012). This is in contrast to the increasing body of evidence in the British Isles (Fabel et al., 2002; Ballantyne and Stone, 2015; and references therein) and Scandinavia (e.g. Hättestrand and Stroeven, 2002) that relates the late Pleistocene periglacial trimline to an englacial thermal boundary

* Corresponding author.
E-mail address: jerzyzasadni@geol.agh.edu.pl (J. Zasadni).

http://dx.doi.org/10.1016/j.quascirev.2016.05.001
0277-3791/

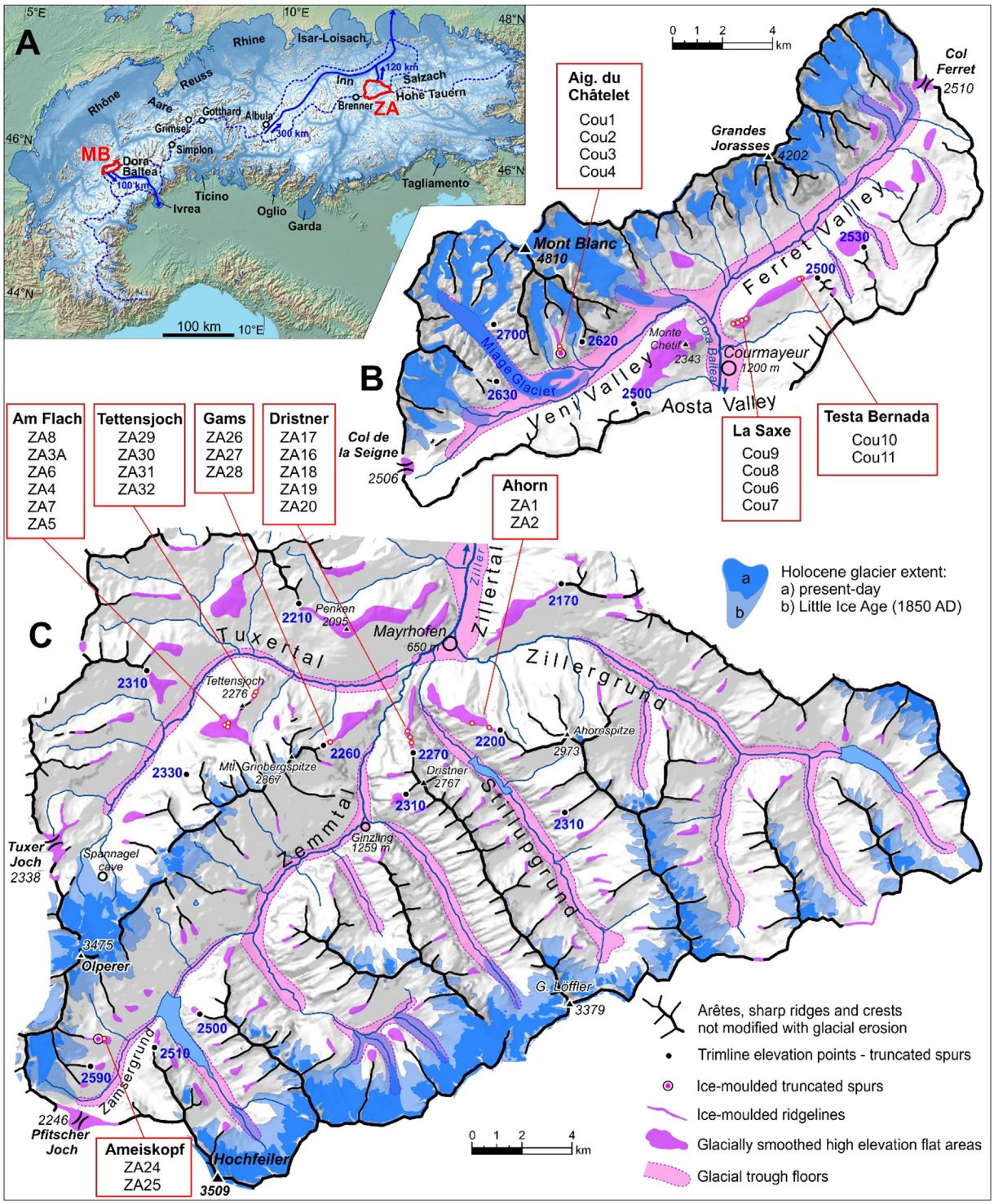

Fig. 1. A) The Alps during the Last Glacial Maximum with locations mentioned in the text. The red outlines mark the locations of the two study areas: MB = Mont Blanc, ZA = Zillertal Alps. The blue arrows show the course of the Dora Baltea and Inn Glacier to their piedmont lobes. Blue dashed lines show main Alpine water divide and extent of the Aosta (Dora Baltea) and Inn Valley systems. The ice extent is from Ehlers and Gibbard (2004, http://www.qpg.geog.cam.ac.uk/lgmextent.html, accessed 20.11.2015). B, C) Simplified geomorphological maps of the MB and ZA study areas, respectively. Samples are arranged by elevation within each sampling site. (For interpretation of the references to colour in this figure legend, the reader is referred to the web version of this article.)

between cold-based ice above and erosive warm-based ice below. In particular, glacial erratic boulders perched on periglacial blockfields far above the trimline show young LGM or post-LGM exposure ages; thus the periglacial zone had to have been overridden by cold-based ice during the last glaciation (Fabel et al., 2002; Ballantyne and Stone, 2015). No such evidence has been presented for the Alps.

The timing of the transition of the Alps from the LGM to its present state has been intensely studied (Schlüchter and Röthlisberger, 1995; Ivy-Ochs et al., 2004; Ivy-Ochs, 2015, and

references therein). Most available data are from the forelands, where fluctuations of the ice margin are better recorded than elevation changes of the ice surface in the High Alps. The outermost positions in the Italian morainic amphitheaters were occupied until 24–23 ka (Monegato et al., 2007; Gianotti et al., 2008, 2015; Ravazzi et al., 2012; Fontana et al., 2014; Scapozza et al., 2015). Withdrawal from the maximum positions of major lobes in the northern Swiss foreland (Rhône, Aare, Reuss) appears to have occurred simultaneously (Ivy-Ochs et al., 2004; Akcar et al., 2011; Reber et al., 2014; Graf et al., 2015; Ivy-Ochs, 2015). Subsequently, a second LGM advance phase is recognized on both sides of the Alps ending around 21–19 ka, followed by retreat of the glacier lobes from the forelands (Lister, 1988; Monegato et al., 2007; Starnberger et al., 2011; Ravazzi et al., 2012; Fontana et al., 2014; Reber et al., 2014). A re-calculation and re-interpretation of exposure ages revealed a similar chronology in the Italian Maritime Alps (Federici et al., 2012, 2016; Ivy-Ochs, 2015). In Austria, it has been suggested that inner-Alpine valleys were ice free as early as 19 ka (Klasen et al., 2007; Reitner, 2007) due to a catastrophical collapse of the foreland tongues (van Husen, 2000; Reitner, 2013).

Comparably little chronological information is available from the High Alps. Wirsig et al. (2016) report that the highest ice surface in the Oberhasli (CH) appears to have been maintained until 23 ± 1 ka. Severe ice surface lowering initiated at Simplon pass (CH) and in the Oberhasli at ~ 18 ka (Dielforder and Hetzel, 2014; Wirsig et al., 2016). Other passes in Switzerland - Grimsel, Gotthard and Albula - show no signs of deglaciation before 16–14 ka (Kelly et al., 2006; Böhlert et al., 2011; Hippe et al., 2014). The authors suggest that the time lag to the retreat of ice from the forelands was caused by local ice that persisted on the passes, which remained in the accumulation area during most of the Lateglacial. The first major glacier re-advance during the Gschnitz stadial was dated to 17–16 ka (Ivy-Ochs et al., 2006a). Mass movement deposits underlying the Gschnitz till are evidence of previously ice-free valleys within the Alps (van Husen, 1997). Therefore, the LGM glaciers had disappeared before the Gschnitz stadial (Kerschner et al., 1999; Schmidt et al., 2012).

This study aims to contribute to the development of a more detailed understanding of the deglaciation chronology in the High Alps. In particular, we investigate whether ice surface lowering at the centers of ice accumulation was synchronous to the retreat of piedmont lobes from the forelands. We address this question by interpretation of exposure ages from boulder and bedrock surfaces from locations at slightly lower elevations than the LGM ice surface in two study areas: one at the southern side of the Mont Blanc in the Western Alps, the other in the Zillertal Alps in the Eastern Alps (Fig. 1A). These areas are subject to rather different climate regimes today: while the Mont Blanc area is dominated by prevailing Westerlies, Zillertal is under a stronger continental influence. Did deglaciation in the two areas, which are separated by 600 km W - E and oriented towards different sides of the main Alpine divide, start at the same time?

2. ^{10}Be surface exposure dating

Due to the predictable build-up with time, the concentration of cosmogenic nuclides such as ^{10}Be in a rock surface carries information of how long it has been exposed to cosmic rays. This is routinely used to date the deposition age of landforms such as moraines, fluvial terraces or landslides (Gosse and Phillips, 2001; Bierman et al., 2002; Ivy-Ochs and Kober, 2008, and references therein). The ^{10}Be concentration in previously glacier-covered bedrock has been studied to determine the time since the ice disappeared (e.g. Ivy-Ochs, 1996; Kelly et al., 2004; Ivy-Ochs and Briner, 2014; Hughes et al., 2016a).

2.1. Sampling strategy

The sample campaigns in both study areas were prepared by a thorough pre-analysis of possible sites. Based on field evidence, interpretation of maps and DEMs and the survey of existing reconstructions of the LGM ice surface we identified sample site candidates. We aimed for sites 1) that were as close as possible below the reconstructed LGM ice surface, 2) that were outside the known extent of any Lateglacial glacier readvance, 3) where topography reduces the risk of long-lasting snow or local ice fields, 4) that contain bedrock outcrops or boulders of a suitable (i.e. quartz-bearing) lithology and 5) that are accessible both from the perspectives of logistics and safety.

Applying these criteria led to the targeting of two types of landforms: 1) narrow ridges just below the trimline (Fig. 2A) and 2) glacially smoothed high elevation flat areas (Fig. 2B). Within a trough, narrow ridges below truncated spurs are ideal sampling spots to address the questions posed in this study. The relative position to the LGM ice surface is well-constrained due to the proximity to the trimline. Furthermore, an ice surface at comparable elevation can only be attained by a glacier system of LGM-like size, which excludes interference caused by Lateglacial stadials. It has to be examined carefully, however, whether glaciers from nearby tributary valleys or cirques could have extended over the sampling spots (Ivy-Ochs, 1996; Kelly et al., 2004; Ivy-Ochs et al., 2007; Hippe et al., 2014). In contrast, high-elevation areas that were clearly below the LGM ice surface (judged by morphology and position in the valley) qualify as sampling site candidates only if there is no accumulation zone above that could support a glacier reaching out onto the site. Keeping this in mind, we focused on convex areas, in particular ridges and bedrock highs within the glacial trough. As the complete ridge or bedrock high was buried by LGM ice in these cases, there is no local trimline evidence. Therefore one has to rely on a wider-scale ice surface reconstruction to estimate how thick the ice cover at the sample site was. Furthermore, it has been suggested that local patches of ice can persist in similar settings, high elevation transfluence passes and trough-shoulders, throughout the Lateglacial until the Bølling-Allerød interstadial (Böhlert et al., 2011; Wirsig et al., 2016). This type of ice cover is also conceivable on ridges below the trimline, if they are not as narrow as in Fig. 2A (Aiguille du Châtelet site).

Within each site candidate, suitable sampling spots were chosen to minimize cover by annual snow. If boulders of sufficient size (>1 m) were present they were preferred as they are thought to stick out of the snow. Otherwise we targeted the top of the highest bedrock outcrops, preferably close to steep drops in elevation (Fig. 2C and D). To constrain the uncertainty introduced by unknown erosion rates, severely weathered rock surfaces were avoided. Some quartz veins displayed glacial polish that indicates negligible weathering. In the absence of clearly polished surfaces we selected bedrock that formed a coherent surface consistent with being ice-moulded. Quartz veins were sampled where available. We collected the uppermost 1.0–4.0 cm thick layer of the rock surface with hammer, chisel and a battery-powered saw.

2.2. Sample preparation, measurement and age calculation

The method of Beryllium sample preparation is comprehensively described in the literature (e.g. Kohl and Nishiizumi, 1992; Ivy-Ochs, 1996). We use grain sizes <1 mm of quartz separates. The addition of a commercial ^{9}Be carrier is followed by quartz dissolution in HF and Be purification using ion-exchange columns and selective precipitation. The ^{10}Be/^{9}Be ratio is measured by

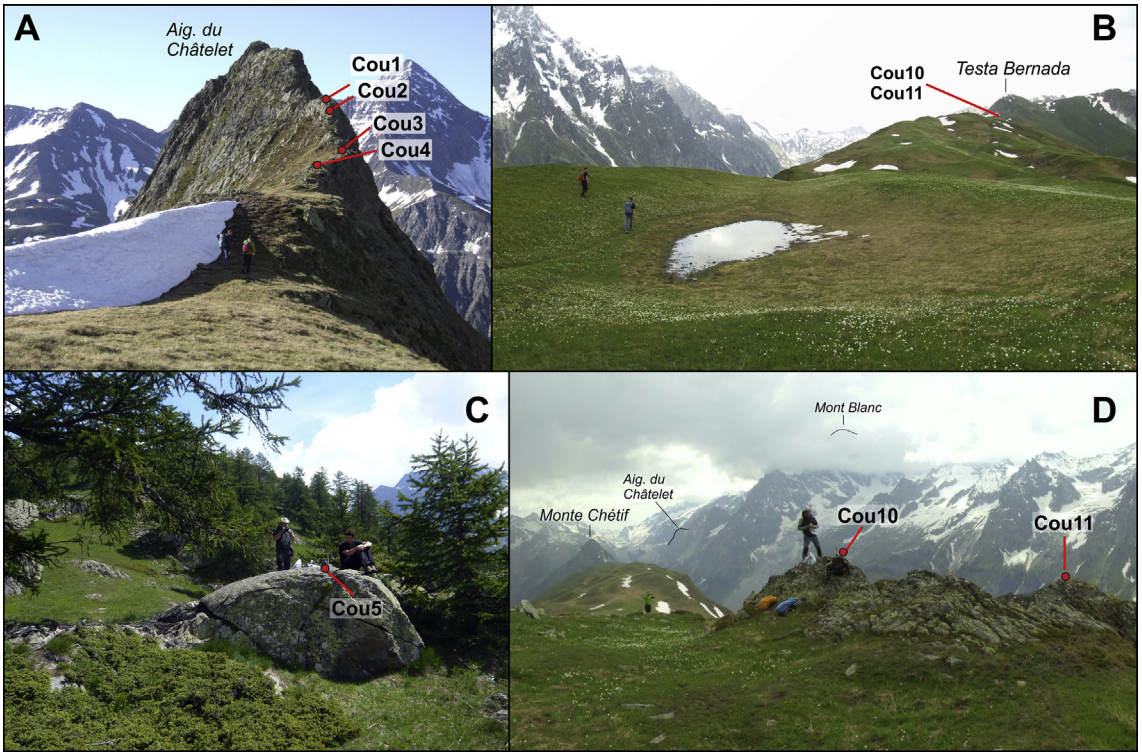

Fig. 2. Pictures from sites in the Mont Blanc study area. A) Aiguille du Châtelet: an ice-moulded truncated spur. View is downhill from the tributary into the Veni trough valley. Note the adverse slope at the spur end. B) Glacially smoothed high elevation area between the sampling sites La Saxe and Testa Bernada. C) Sample Cou5 at site La Saxe. D) Samples Cou10 and Cou11 at site Testa Bernada. Note humans on each picture for scale.

accelerator mass spectrometry (AMS) on the 600 KV TANDY system at the Laboratory of Ion Beam Physics (LIP) at ETH Zürich against the in house standard S2007N (Christl et al., 2013) that is calibrated against the 07KNSTD standard (Nishiizumi et al., 2007). We correct for a long-term average full chemistry procedural blank of $^{10}Be/^{9}Be = (3.6 \pm 2.6) * 10^{-15}$. Ages were calculated using the production rate of Balco et al. (2009): 3.87 ± 0.19 at/g/a at sea level and high latitude (SLHL) and 'Lm' scaling, with the CRONUS-EARTH online calculator (Balco et al., 2008). Erosion rates of 0.1 mm/ka were applied for bedrock, 1 mm/ka for boulder samples. This takes into account the observed difference in surface weathering. The reported errors propagate uncertainties from AMS standard reproducibility, counting statistics, standard mean error of samples, blank correction and the local production rate value. These external errors are used to compare absolute ages to independent chronologies. Internal errors ('int.') exclude the uncertainty of the local production rate. All errors are reported on the 1σ level.

Following the argument given in Wirsig et al. (2016), we apply a snow correction of 50 cm for 6 months per year to all bedrock samples. To reflect our sample preference for exposed locations on bedrock high, these values are chosen low compared to average snow cover in the study areas in the past decade which are >100 cm for 6 months per year based on reports of local ski areas. We exclude samples from the Aiguille du Châtelet site from this correction, because the steep wall of the ice-moulded truncated spur does not offer any space for snow accumulation (see Fig. 2A). Furthermore, no snow correction is applied to boulder samples. The correction factor is calculated following eq. (3.76) in Gosse and Phillips (2001) with a snow density of 0.3 g/cm^3 and an attenuation length for fast neutrons in snow of 109 g/cm^2 (Zweck et al., 2013; Delunel et al., 2014; Dunai et al., 2014). This reduces spallogenic production rates by ~6.4% (cf. Schildgen et al., 2005).

3. Study areas

This work has been performed in two study areas (Fig. 1). One is an area of 20 km * 25 km on the Italian side of the Mont Blanc massif. The other is the Zillertal Alps in Austria, a 30 km * 35 km area of northward trending valleys. The two areas are approximately 600 km apart on the Alpine divide, mainly in an W-E direction. Their orientation with respect to the main mountain chain puts them on opposite sides of the weather divide: the Mont Blanc study area to the south, Zillertal Alps to the north. At an average of 6.3 °C and 1139 mm annual precipitation, Courmayeur (1261 m) near the Mont Blanc is approximately 1 °C warmer and 30% moister than Ginzling (1259 m, 5.2 °C, 896 mm) near Mayrhofen in Zillertal (http://en.climate-data.org/, accessed 16.12.2015). Whereas the precipitation in Courmayeur is distributed evenly over the year, Ginzling in Zillertal is characterized by wetter summers and drier winters with 40–50 mm precipitation per month on average.

3.1. Mont Blanc

The Mont Blanc massif is located in the Western Alps at the borders of France to the NW, Italy to the SE and Switzerland to the E. The study area is at its south-eastern flank that consists mainly of granites, gneisses and mica schists forming very steep walls (Pfiffner, 2014, and references therein). The Veni and Ferret Valleys (Fig. 1B) mark the contact to the metasedimentary rocks connecting to the massif towards the south that form lower and gentler terrain. Crystalline rocks crop out at only three places on the adjacent range of hills to the immediate south. The crystalline summit of Testa Bernada (2534 m) is part-way up the Ferret Valley. Monte Chétif (2343 m) and the slope at La Saxe at the end of Veni and Ferret Valleys, respectively, are separated by the town of Courmayeur at the head of the Aosta Valley (Fig. 1B). Here, at the junction of the

Veni and Ferret Valleys is where the Dora Baltea River drains towards the south.

Approximately 30% of the massif's 550 km^2 area are glacierized today due to its high elevation that includes Europe's highest summit, the Mont Blanc at 4810 m (Deline et al., 2012). The area has received high interest since the beginning of the study of Quaternary glaciations (de Saussure, 1779–1796). Penck and Brückner (1901/1909) devised a general framework of Alpine glaciations that included the attribution of the Ivrea Amphitheater to the maximum extent of the Dora Baltea Glacier. Gianotti et al. (2008, 2015) conducted intensive research at the Ivrea Amphitheater which was the terminus of the LGM as well as several previous Quaternary glaciations. The LGM ice surface around the Mont Blanc massif itself has been described by multiple authors through trimline mapping with diverging results. Porter and Orombelli (1982) and Coutterand and Buoncristiani (2006) reconstruct the ice surface at Courmayeur at 2600 m, 200 m higher than Kelly et al. (2004) and Bini et al. (2009). The offset remains constant up to the heads of the steep tributary valleys at the Mont Blanc SE face.

Lateglacial deposits are rarely encountered on the Aosta Valley floor, as this is thickly covered by alluvium and rockfall deposits (Porter and Orombelli, 1982). Gianotti et al. (2008, 2015) discuss the evidence for seven locations of Lateglacial stadial advances along the Aosta Valley, upvalley of the Ivrea Amphitheater. A constraint on the ice surface within our study area is only available for two of the potential terminal positions, however. Based on the upper limit of erratic boulders along the Ferret and Veni Valleys, Porter and Orombelli (1982) reconstruct the ice surface of an advance with a terminal position close to Courmayeur. The limit of the smaller Planpincieux advance is determined by mapping of moraines and outwash deposits (Porter and Orombelli, 1982). Surface exposure ages from a roche moutonnée 80 km downvalley from Courmayeur are 17–16 ka (Gianotti et al., 2008, 2015), synchronous to ages determined for the Gschnitz stadial (Ivy-Ochs et al., 2006a). The ice surface in our study area for this readvance is unknown.

We selected three sampling sites in the Mont Blanc study area (Fig. 1B). The Aiguille du Châtelet (2525 m) is located at the southern wall of the Mont Blanc, 750 m above the current terminus of Miage Glacier in the Veni Valley (Fig. 2A). It is a narrow ridge on a truncated spur in between the Frêney and Brouillard Glacier. Its smooth western slope has clearly been moulded by the LGM Veni Glacier moving from W to E. Trimlines on adjacent spurs at ~2650 m indicate that Aiguille du Châtelet was covered by 100–150 m of ice during the LGM. It has an adverse slope at its end and a local relief to the adjacent glacier beds of >400 m. Glaciers of this thickness in the steep tributary valleys can be excluded during any of the Lateglacial readvances based on estimated terminal positions (Gianotti et al., 2008, 2015). A line of boulders uphill on the ridge potentially marks the extent of a Lateglacial glacier advance well outside the reach of the end of the spur where we sampled. Aiguille du Châtelet is therefore expected to have become and continue being exposed once the LGM ice surface in Veni Valley lowered by more than ~150 m. Here we took four bedrock samples (Cou1-4) from the crest of the sharp ridge a few meters from the top towards the direction of the tributary valleys.

The site at La Saxe is on top of a steep bedrock cliff towering to the east of Courmayeur at the beginning of the Ferret Valley (Fig. 1B). The top is a comparably flat, regular surface with numerous roches moutonnées. It was covered by more than 350 m of ice during the LGM (Porter and Orombelli, 1982; Kelly et al., 2004; Coutterand and Buoncristiani, 2006). Here we collected bedrock samples from two different elevations, separated by a farming area with marked human impact on the landscape. Samples Cou6,7 from the lower elevation range at ~1900 m are 700 m above the present Aosta valley floor and 600 m above the reconstructed ice surface of the Courmayeur advance (Porter and Orombelli, 1982). The locations of Cou8,9 are at ~2000 m. We targeted the top of the highest well-preserved roches moutonnées that stood 1–2 m above the surrounding topography (Fig. 2C).

Following the same ice-moulded high elevation area to the east, the third sample site is a granite outcrop at the foot of Testa Bernada. Depending on which LGM ice surface reconstruction is consulted, this spot was covered by 50 m (Kelly et al., 2004; Bini et al., 2009) to 250 m of ice (Porter and Orombelli, 1982; Coutterand and Buoncristiani, 2006). The general morphology is smooth, but irregular with indentations where snow fields persist until late summer (Fig. 2B). Despite a considerable degree of weathering, the bedrock preserved general stoss and lee features. We collected two samples (ZA10,11) where the bedrock stood 1–2 m above the surrounding topography (Fig. 2D). We did not sample any quartz veins or polished rock surfaces at Mont Blanc.

3.2. Zillertal Alps

The Zillertal Alps massif is located in the Eastern Alps between Brenner Pass to the W and the Hohe Tauern mountain range to the E (Fig. 1A). The main crest of the massif is formed by a range of peaks with summits above 3000 m that is part of the main Alpine water divide and constitutes the Austrian - Italian border. The highest peaks are Hochfeiler (3509 m) and Olperer (3476 m) that form a relief of ~2000 m to the adjacent valley floors. The northern slope of the Zillertal Alps is dissected by a system of four principal tributary valleys: Tuxertal, Zemmtal, Stillupgrund and Zillergrund that merge in one point near Mayrhofen (Fig. 1C). From there the Ziller River drains towards the north into the Inn River.

The highest part of the Zillertal Alps is built of weathering-resistant rocks of the crystalline core of the Tauern Window, Zentralgneis (Frisch, 1980; Veselá et al., 2008). In Tuxertal, a variety of metasedimentary and metavolcanic rocks stacked in the Venediger nappes outcrop in the south, whereas the north is formed by Bündnerschiefer of the Glockner nappes (Froitzheim et al., 2008, and references therein). The marked difference in relief and preservation of glacial erosional landforms (troughs, cirques, arêtes) is due to the resistant gneisses found in the southern part of the study area compared to weaker lithologies encountered towards the north (Penck and Brückner, 1901/1909; Bobek, 1933).

Geomorphological mapping of the area at a scale 1: 10,000 was performed over the course of ten years by J. Zasadni as an assignment from the Geological Survey of Austria (Geologische Bundesanstalt Wien, GBA). Particular emphasis was put on mapping of glacial landforms and trimlines that enabled a reconstruction of the LGM ice surface and identification of Lateglacial stadial extents (Zasadni, 2010, 2011). A simplified version of the geomorphological map is shown in Fig. 1C. The focus of this study is on the southern part of the Zillertal Alps, quoted many times as a text-book example of High Alpine glacial relief (e.g. Penck and Brückner, 1901/1909; Heuberger, 1968; Louis and Fischer, 1979). Whereas Tuxertal and Stillupgrund are simple glacial troughs, Zemmtal and Zillergrund constitute a dendritic network of well-developed troughs with tributary hanging valleys (Penck, 1905).

Together with the Hohe Tauern mountain range, the Zillertal Alps formed a dominant center of accumulation of the Eastern Alpine transection glaciers during the Last Glacial Maximum (van Husen, 1987). The LGM Ziller Glacier joined the Inn Glacier system that extended into the northern Alpine foreland. The Inn Valley system is a type region of the 'Würm' glaciation in the Alps as defined by the Subcommission of European Quaternary Stratigraphy (Chaline and Jerz, 1984). Original localities of the Lateglacial stadials Gschnitz and Egesen are located in this area (Kerschner, 1986; Ivy-Ochs et al., 2006b, and reference therein). In the

Hopfgarten area, part of the Inn Valley system 50 km downvalley from the Zillertal Alps, morphological and sedimentary evidence indicates a phase of early Lateglacial ice decay of the Inn Glacier that followed the full LGM condition and preceded the Gschnitz stadial (Reitner, 2007).

The LGM ice surface in the study area has been reconstructed by several authors (Penck and Brückner, 1901/1909; Mayr and Heuberger, 1968; van Husen, 1987). Moraines near Mayrhofen and in the middle section of Tuxertal were tentatively correlated to the Lateglacial Gschnitz readvance (Penck and Brückner, 1901/1909; Bobek, 1932). Recent mapping results (e.g. Zasadni, 2014) indicate that large dendritic Gschnitz glaciers almost entirely occupied four principal tributary valleys around Mayrhofen (Fig. 3A). Moraines that were attributed to the Egesen stadial are mostly on the mountain slopes and cirques; the glaciers with the largest accumulation areas reached the valley floors, e.g. from Pfitscherjoch to Zamsergrund (Bobek, 1932; Heuberger, 1977). Climate reconstructions from the Spannagel cave in Tuxertal based on speleothem records yield detailed information on local paleotemperatures, in particular during the Holocene (Vollweiler et al., 2006; Fohlmeister et al., 2013), but also for the more distant past (Spötl and Mangini, 2006, 2007).

We selected six sampling sites in the Zillertal study area. Differences in elevation to the LGM ice surface are based on an interpolation of mapped trimline data (Fig. 1C) which indicate an ice surface elevation above Mayrhofen and in the lower section of tributary valleys of ca. 2200 m and 2300 m, respectively. Three sample sites are on different ridges close to the confluence area at Mayrhofen (Fig. 3A): Gams (ZA26-28), Dristner (ZA16-20) and Ahorn (ZA1,2). The LGM ice surface is tightly constrained by truncated spurs on each ridge that mark the local trimline. We aimed to collect samples at the highest elevation with suitable bedrock outcrops, since no boulders were available. The Gams and Ahorn sites are relatively broad, covered with low vegetation that is interrupted by several meter high outcrops of weathered Zentralgneis. Glacial polish is preserved on quartz veins that we preferably sampled. A lateral moraine in the forest ~1000 m below the Ahorn site is correlated to the Gschnitz readvance (Zasadni, 2014). The Dristner site is on the sharpest of the three ridges. The two topmost samples (ZA17,16) are from a sparsely vegetated area less than 100 m below the trimline where glacially moulded Zentralgneis forms a steep and narrow ridge. Three additional samples were taken in steps of ~100 m altitude (ZA18-20) to look at the rate of ice surface lowering. The ridge broadens with decreasing altitude and vegetation becomes denser.

Two sites, Am Flach and Tettensjoch, are on opposite slopes on the same ridge in Tuxertal. The sites were covered by ca. 100 m of ice during the LGM as inferred from nearby trimline elevation points (Fig. 1C). The upstream SW slope of the Am Flach site is gentle and flat. It hosts 14 erratic Zentralgneis boulders with an a-axis size between 0.7 m and 14 m. We sampled four of the largest well-preserved boulders (ZA3A,4,5,8; Fig. 3B) and two bedrock outcrops (polished quartz veins, ZA6,7). At Tettensjoch on the NE side of the ridge pointing downstream towards Mayrhofen, steps of fractured bedrock form a steeper and narrower slope than at Am Flach, sometimes preserving a roche moutonnée shape. Here we targeted the sharp edge of the ridge and bedrock knobs next to steep drops for collecting four bedrock samples (ZA29-32).

Sample site Ameiskopf is located 18 km upvalley in Zemmtal. Similar to the Aiguille du Châtelet site in the Mont Blanc study area, it is an ice-moulded truncated spur at the end of a ridge that separates two tributary cirques. The elevation difference to the adjacent cirque floors is 200–300 m. Here the orientation of the sampling site is different than at Aiguille du Châtelet, however. The Ameiskopf site is located directly beneath the spur towards the main trough, not behind the spur towards the cirques. The trough-side of the spur where we sampled is narrow, but flat and smooth. The bedrock there shows abundant evidence of onion-type exfoliation weathering. We therefore targeted spots with quartz veins that preserved glacial polish. The two samples (ZA24,25) were taken only few centimeters from the steep and deep drop that limits the side of the flat area.

4. Results and interpretation

Sample information and measured ^{10}Be concentrations of the 32

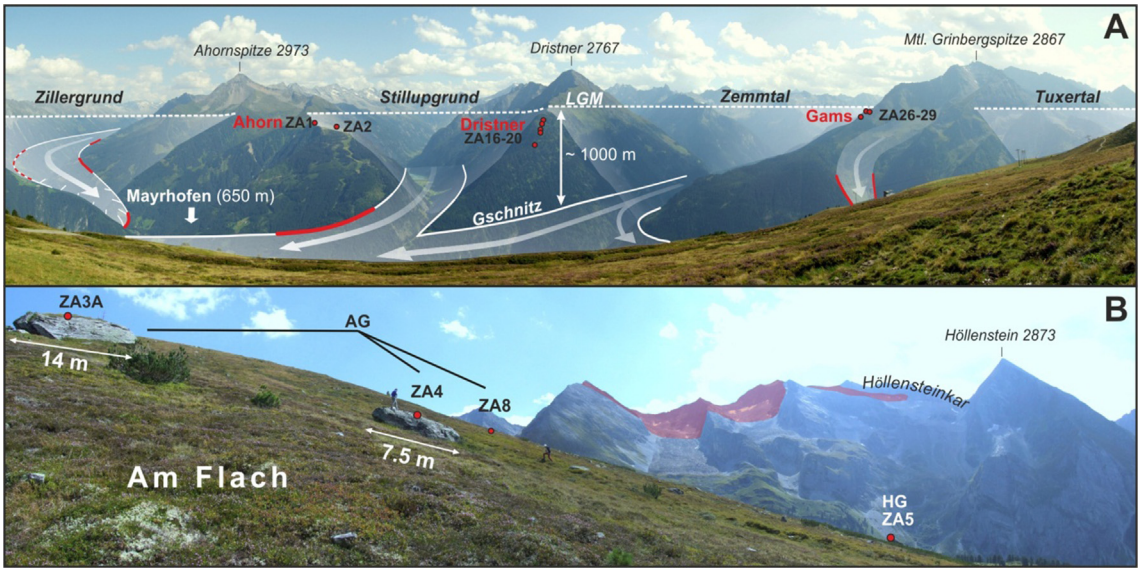

Fig. 3. Sample positions in the Zillertal Alps. A) Ahorn, Dristner and Gams sites with respect to the reconstructed LGM and Gschnitz stadial ice surfaces. Red dots are sample positions, red lines moraines, white lines reconstructed ice surfaces. The photograph is taken from Penken mountain (2095 m), view to the SSW. Ice flow was out of the valleys towards the confluence at Mayrhofen. The Am Flach and Tettensjoch sites are just out of view in Tuxertal. Ameiskopf is located upvalley in Zemmtal. B) Sampled erratic boulders at the Am Flach site. Boulders were transported 3 km from Höllensteinkar where their source lithology occurs (red layer); Ahorn gneiss (AG; boulders: ZA3A, ZA4 and ZA8) and Höllenstein gneiss (HG: boulder ZA5). Note person on ZA4 for scale. (For interpretation of the references to colour in this figure legend, the reader is referred to the web version of this article.)

samples are summarized in Table 1. Tables 2 and 3 list calculated exposure ages with and without snow correction and associated uncertainties for the Mont Blanc and Zillertal Alps study area, respectively. The snow corrected exposure ages will be used for the interpretation and discussion. First we present the age patterns within each study area, then point out implications in the discussion section.

4.1. Mont Blanc

The obtained ages from ten samples in the Mont Blanc study area range from 14.2 ± 1.0 ka to 18.5 ± 1.1 ka (Table 2, Fig. 4A). The two oldest ages are from Cou3 and Cou1 at the Aiguille du Châtelet site on the northern side of Veni Valley. Due to the sharp ridge, adverse slope and high elevation difference to the adjacent glacier beds, we consider there is no possibility of temporary ice cover. Furthermore, there is no place for annual snow to accumulate on the narrow ridge crest (Fig. 2A). The age of Cou3 (18.5 ± 1.1 ka) is therefore interpreted as the onset of ice surface lowering in Veni Valley. The younger age of Cou4 must relate to spalling of the original surface that was undetected due to the generally weathered character of the ridge crest.

Our interpretation of trimline evidence at the Aiguille du Châtelet is within the range of previous reconstructions. Fig. 4A shows the relative position of the sampling site to the LGM ice surface constrained by the trimlines on the adjacent truncated spurs. On the spur to the east, we place the trimline at 2620 m, 50 m higher than some authors (Kelly et al., 2004; Bini et al., 2009), but 150 m lower than others (Porter and Orombelli, 1982; Coutterand and Buoncristiani, 2006). On the southern slope of Ferret Valley, our trimline point at 2500 m at Testa Bernada displays the same pattern of differences to previous reconstructions. Since we do not generate a comprehensive reconstruction of the LGM ice surface in the Mont Blanc study area, we calculate the elevation difference of individual sample spots to the ice surface in the map of Bini et al. (2009), because it appears more similar to our interpretation. Due to the constant offset between different reconstructions, the relative distribution of elevation differences to the LGM ice surface is conserved if another reconstruction is selected as reference.

The two samples at Testa Bernada (Cou10,11) yield congruent ages of ~16.4 ka. Likewise, the four ages from La Saxe (Cou6-9) are very consistent at 14.7–15.8 ka. These ages from the southern side of the Ferret Valley show an evident mismatch to the onset of LGM ice surface lowering at the Aiguille du Châtelet site of 2–3 ka. A delayed lowering of the LGM ice surface by 2–3 ka in the Ferret Valley, compared to the Veni Valley, is not possible, however; due to their immediate confluence at Courmayeur, the ice surfaces of the LGM trunk glaciers in the two valleys depended on the position of the same glacier tongue in the Aosta Valley and must behave synchronously. Samples from the Testa Bernada site should therefore reflect exposure simultaneous to or even before ~18.5 ka (Cou3), because they were closer to the ice surface than the Aiguille du Châtelet. The age mismatch indicates temporary cover by ice or sediment after the LGM ice surface dropped. Indeed, the irregular topography on the La Saxe ridge with rounded indentations (Fig. 2B) offers plenty of opportunities for local patches of ice to form and persist, given sufficiently cold conditions as for example during the Lateglacial. Despite our careful selection of sample sites we

Table 1
Sample list and measured ^{10}Be concentrations.

Sample ID	Latitude	Longitude	Elevation	Thickness	Topographic shielding factor	^{10}Be conc.
	WGS 84		*m a.s.l.*	*cm*		*10^5 at/g_{qtz}* [a]
			Mt. Blanc			
Cou1	45.7958	6.8843	2500	4.0	0.967	4.75 ± 0.14
Cou2	45.7958	6.8843	2497	1.0	0.959	4.34 ± 0.17
Cou3	45.7961	6.8841	2488	3.0	0.958	4.89 ± 0.15
Cou4	45.7961	6.8844	2477	2.0	0.888	3.46 ± 0.16
Cou6	45.8079	6.9739	1913	2.0	0.992	2.74 ± 0.17
Cou7	45.8080	6.9740	1912	3.0	0.987	2.56 ± 0.10
Cou8	45.8099	6.9800	2016	2.0	0.986	2.71 ± 0.11
Cou9	45.8100	6.9792	2027	4.0	0.990	2.84 ± 0.12
Cou10	45.8243	7.0091	2402	3.5	0.992	3.94 ± 0.16
Cou11	45.8241	7.0091	2401	2.5	0.996	3.96 ± 0.31
			Zillertal Alps			
ZA1	47.1334	11.8781	2076	2.5	0.968	3.54 ± 0.20
ZA2	47.1346	11.8674	1917	1.5	0.992	2.84 ± 0.15
ZA3A	47.1374	11.8698	2176	3.5	0.995	3.39 ± 0.33
ZA4	47.1371	11.7361	2168	1.5	0.992	3.31 ± 0.18
ZA5	47.1361	11.7356	2143	2.0	0.992	3.37 ± 0.16
ZA6	47.1377	11.7363	2172	1.5	0.971	3.63 ± 0.12
ZA7	47.1376	11.7360	2165	2.0	0.975	3.15 ± 0.13
ZA8	47.1366	11.7373	2192	4.0	0.994	3.40 ± 0.16
ZA16	47.1276	11.8342	2122	2.5	0.945	3.29 ± 0.16
ZA17	47.1276	11.8349	2130	1.5	0.914	3.46 ± 0.18
ZA18	47.1298	11.8350	2039	2.0	0.995	3.09 ± 0.18
ZA19	47.1306	11.8338	1988	2.5	0.978	2.98 ± 0.13
ZA20	47.1325	11.8325	1834	2.0	0.968	2.47 ± 0.12
ZA24	47.0231	11.6671	2465	2.0	0.972	3.78 ± 0.12
ZA25	47.0231	11.6671	2463	1.5	0.978	3.92 ± 0.17
ZA26	47.1281	11.7901	2223	1.5	0.988	3.73 ± 0.13
ZA27	47.1282	11.7899	2221	1.0	0.985	3.25 ± 0.24
ZA28	47.1285	11.7909	2172	1.5	0.954	3.05 ± 0.13
ZA29	47.1474	11.7536	2126	1.0	0.987	3.35 ± 0.19
ZA30	47.1474	11.7538	2115	1.0	0.944	3.46 ± 0.13
ZA31	47.1478	11.7539	2108	1.5	0.995	3.24 ± 0.17
ZA32	47.1479	11.7542	2089	1.5	0.988	3.68 ± 0.58

[a] Measured against standard 07KNSTD (Nishiizumi et al., 2007), corrected for full process blank of (3.6 ± 2.6) * 10^{-15} ^{10}Be/^{9}Be.

Table 2
Sample type and ages from the Mt. Blanc study area, arranged by difference in elevation to the reconstructed LGM ice surface and grouped to sampling sites.

Sample ID	Δ elevation to LGM[a]	Elev.	Type	Site (elevation of ice surface)	^{10}Be exposure age[b]		
					no correction		incl. snow corr.[c]
	m	*m a.s.l.*			*ka*	± (*int.*)	*ka*
Cou10	−48	2402	Bedrock	Testa Bernada	15.4 ± 1.0	0.6	16.4 ± 1.0
Cou11	−49	2401	Bedrock	(2450 m)	15.3 ± 1.4	1.2	16.3 ± 1.5
Cou1	−80	2500	Bedrock		17.8 ± 1.0	0.5	
Cou2	−83	2497	Bedrock	Aiguille du Châtelet	16.1 ± 1.0	0.7	
Cou3	−92	2488	Bedrock	(2580 m)	18.5 ± 1.1	0.6	
Cou4	−103	2477	Bedrock		14.2 ± 1.0	0.7	
Cou9	−353	2027	Bedrock		14.5 ± 0.9	0.6	15.4 ± 1.0
Cou8	−364	2016	Bedrock	La Saxe	13.8 ± 0.9	0.6	14.7 ± 0.9
Cou7	−468	1912	Bedrock	(2380 m)	14.1 ± 0.9	0.5	15.0 ± 0.9
Cou6	−467	1913	Bedrock		14.8 ± 1.2	0.9	15.8 ± 1.3

[a] Elevation difference to the LGM ice surface as reconstructed by Bini et al. (2009).
[b] Using NENA production rates of 3.87 ± 0.19 at/g/a (Balco et al., 2009), 'Lm' scaling, erosion rates of 0.1 mm/ka for bedrock and 1 mm/ka for boulder samples. Rock density is 2.65 g/cm^3.
[c] Assuming 50 cm snow for 6 months per year.

Table 3
Sample type and ages from the Zillertal Alps study area, arranged by difference in elevation to the reconstructed LGM ice surface and grouped to sampling sites.

Sample ID	Δ elevation to LGM[a]	Elev.	Type[b]	Site (elevation of ice surface)	^{10}Be exposure age[c]		
					no correction		incl. snow corr.[d]
	m	*m a.s.l.*			*ka*	± (*int.*)	*ka*
ZA26	−27	2223	Bedrock, qtz, p	Gams	15.9 ± 1.0	0.6	17.0 ± 1.0
ZA27	−29	2221	Bedrock	(2250 m)	13.9 ± 1.2	1.0	14.8 ± 1.3
ZA28	−78	2172	Bedrock		14.0 ± 0.9	0.6	14.9 ± 1.0
ZA17	−120	2130	Bedrock, p	Dristner	17.0 ± 1.2	0.9	18.1 ± 1.3
ZA16	−128	2122	bedrock, qtz	(2250–2200 m)	15.8 ± 1.1	0.8	16.9 ± 1.2
ZA18	−201	2039	Bedrock, qtz		15.0 ± 1.1	0.9	16.0 ± 1.2
ZA19	−232	1988	Bedrock, qtz		15.3 ± 1.0	0.7	16.3 ± 1.1
ZA20	−366	1834	Bedrock		14.3 ± 1.0	0.7	15.2 ± 1.0
ZA24	−96	2465	Bedrock, qtz, p	Ameiskopf	14.0 ± 0.8	0.4	14.9 ± 0.9
ZA25	−98	2463	Bedrock, qtz, p	(2560 m)	14.4 ± 0.9	0.6	15.3 ± 1.0
ZA8	−88	2192	Boulder, 0.9 m	Am Flach	15.2 ± 1.1	0.7	
ZA3A	−104	2176	Boulder, 2.4 m	(2280 m)	15.3 ± 1.7	1.5	
ZA6	−108	2172	Bedrock, qtz, p		16.5 ± 1.0	0.6	17.6 ± 1.0
ZA4	−112	2168	Boulder, 1.8 m		14.8 ± 1.1	0.8	
ZA7	−115	2165	Bedrock, qtz, p		14.4 ± 0.9	0.6	15.4 ± 1.0
ZA5	−137	2143	Boulder, 4.5 m		15.4 ± 1.1	0.8	
ZA1	−114	2076	Bedrock	Ahorn	17.4 ± 1.3	1.0	18.6 ± 1.4
ZA2	−273	1917	Bedrock, qtz	(2190 m)	15.2 ± 1.1	0.8	16.2 ± 1.2
ZA29	−134	2126	Bedrock	Tettensjoch	15.3 ± 1.2	0.9	16.3 ± 1.2
ZA30	−145	2115	Bedrock, qtz, p	(2260 m)	16.6 ± 1.0	0.6	17.7 ± 1.1
ZA31	−152	2108	Bedrock		14.9 ± 1.1	0.8	15.9 ± 1.1
ZA32	−171	2089	Bedrock, qtz		17.2 ± 2.9	2.8	18.4 ± 3.1

[a] Elevation difference to the LGM ice surface as reconstructed based on adjacent trimline elevation points.
[b] 'qtz' indicates that a quartz vein was sampled, 'p' indicates a polished surface, 'xx m' gives the boulder height.
[c] Using NENA production rates of 3.87 ± 0.19 at/g/a (Balco et al., 2009), 'Lm' scaling, erosion rates of 0.1 mm/ka for bedrock and 1 mm/ka for boulder samples. Rock density is 2.65 g/cm.^{3}.
[d] Assuming 50 cm snow for 6 months per year.

cannot exclude that these ice patches grew thick and large enough to cover even the highest bedrock outcrops.

The age difference between the Testa Bernada and La Saxe sites possibly reflects the rate of ice surface lowering at the head of the Aosta Valley. This would indicate lowering by 300–450 m in ~1 ka. On the other hand, the lower elevation makes the La Saxe site more likely to be covered during Lateglacial readvances. While the Courmayeur readvance was well below the sampling sites, the ice surfaces of other readvances with terminal positions further down the Aosta Valley are not known. At Testa Bernada, considering the elevation difference of 800 m from the sample spots to the valley floor, it appears highly unlikely that any Lateglacial readvance in Ferret Valley affected the samples. Cover and erosion during Lateglacial advances at La Saxe, however, would decrease the measured nuclide concentrations and result in apparently younger ages.

Chronological data to reference our results are available mostly from the intensive studies of the Ivrea Amphitheater that defined the terminus of the Dora Baltea Glacier during the LGM. ^{10}Be surface exposure ages of 23.8 ± 1.7 ka and 20.1 ± 3.0 ka are interpreted to date the moraine stabilization at the initiation of glacier retreat (Gianotti et al., 2008; recalculated in Gianotti et al., 2015). The amphitheater was completely abandoned by the Dora Baltea Glacier before 17.7–16.8 ka (14.2 ± 1.5 ^{14}C ka (Schneider, 1978)). Before 17–16 ka, the glacier tongue had retreated more than 30 km before depositing a frontal moraine in Torredaniele (Gianotti et al., 2015). Our ages correspond well to this framework: ice surface lowering in the accumulation area starting at 18.5 ka followed after the initiation of, but presumably synchronous to, the retreat of

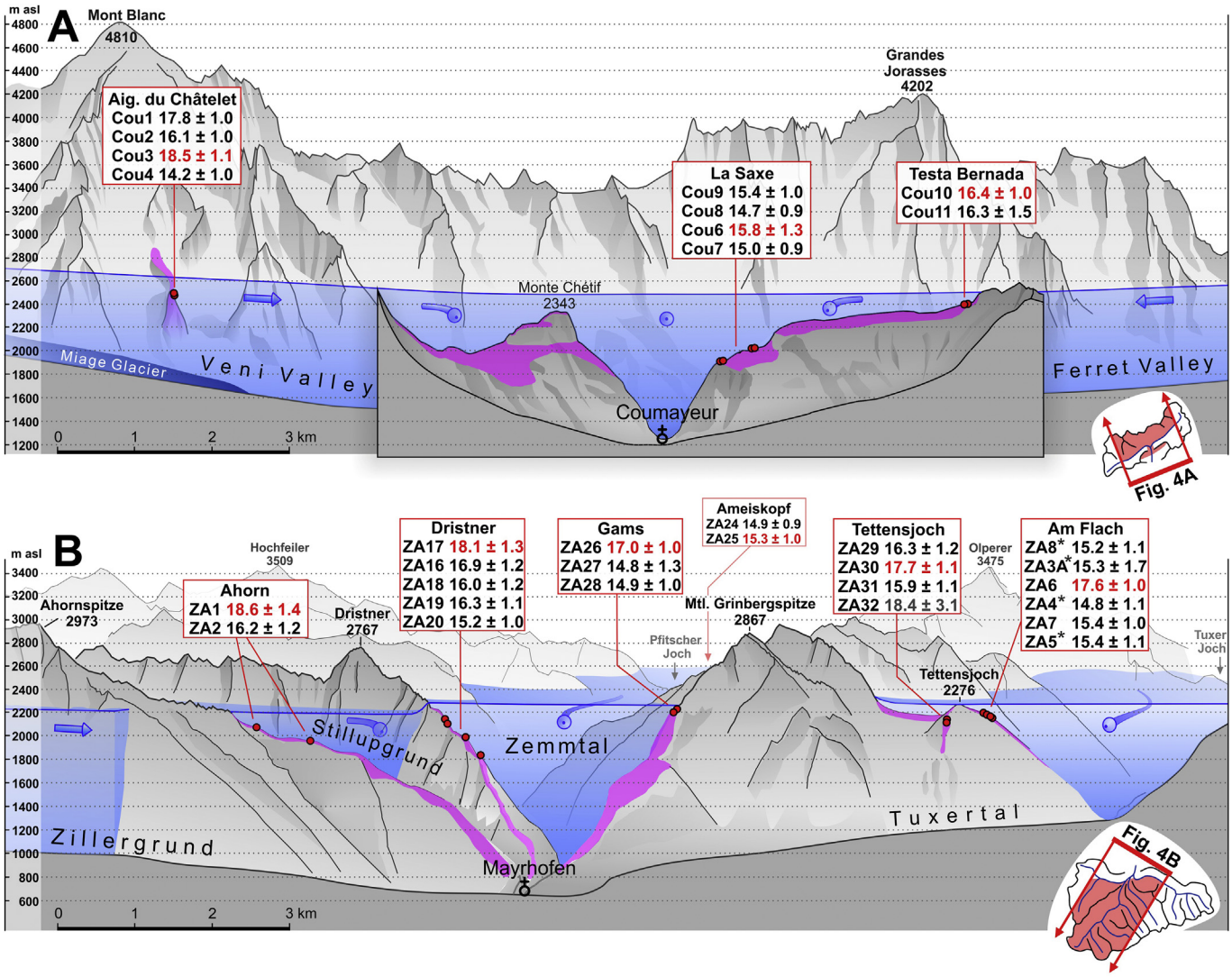

Fig. 4. Surface exposure ages in ka in context with the reconstructed LGM ice surface in the A) Mont Blanc and B) Zillertal Alps study regions. The view is an orthogonal projection of topography. Vertical scale is 1.5x exaggerated. Extent of projections is indicated in the small maps in the bottom right corners that show the outline of the study areas as in Fig. 1. To include all sample sites, two planes of projection are portrayed in panel A. In panel B, the Ameiskopf sample site in the upper Zemmtal Valley is not visible directly. Blue tint and arrows indicate reconstructed LGM ice surface and flow lines. Violet shows ice-moulded ridges, spurs and high elevated flat areas (compare Fig. 1). Exposure ages are arranged by elevation within each sampling site. Red font marks the oldest age at each site. Asterisks show erratic boulder samples. (For interpretation of the references to colour in this figure legend, the reader is referred to the web version of this article.)

significant distances of the Dora Baltea Glacier tongue.

4.2. Zillertal Alps

The obtained ages from 22 samples in the Zillertal Alps range from 14.8 ± 1.1 ka to 18.6 ± 1.4 ka (Table 3). We refrain from the interpretation of ZA32 due to the large uncertainty of 3.1 ka. The oldest ages are from three of the five sites near Mayrhofen (see Fig. 4B): 18.6 ± 1.4 ka at Ahorn (ZA1), 18.1 ± 1.3 ka at Dristner (ZA17) and 17.7 ± 1.1 ka at Tettensjoch (ZA30). We interpret these as minimum ages for the onset of ice surface lowering at the Zillertal confluence basin, which is supported by the good agreement of maximum ages between the individual study sites of ~18 ka. It appears that this is a somewhat delayed reaction to the phase of early Lateglacial ice decay in the Inn Valley of 21.2–19.5 ka (Reitner, 2007) and approximately synchronous first signs of recession of other LGM glaciers in the Eastern Alps (van Husen, 1997; Reuther et al., 2011; Starnberger et al., 2011). The interpretation of our ages is difficult to align with the hypothesis that the lower Inn Valley was ice-free prior to 18 ka (Reitner, 2007, and references therein) as this implies an almost complete melting of the Zillertal tongue compared to the thickness of >1500 m attained during the LGM.

Ages appear to decrease with elevation and therefore distance to the LGM ice surface at some sites, e.g. Dristner and Ahorn. It is thus tempting to interpret the younger ages at lower elevations as tracing the rate of ice surface lowering. Arguing on the basis of individual sites is not correct, however. With the exception of Ameiskopf (ZA24, 25), all sites are strongly connected as they depend on the elevation of the same ice surface in the confluence area near Mayrhofen (Figs. 3A and 4B); they were affected by simultaneous ice surface lowering. Therefore, not individual study sites, but all samples (without ZA24, 25) must be compared to judge if ages decrease with greater elevation distance to the LGM ice surface, as would be expected if they were determined by the rate of ice surface lowering. This is clearly not the case: while the Gams

site was covered by merely 30–70 m of ice and yielded a mean age of 15.6 ± 1.0 ka, the Ahorn site was underneath 110–270 m of ice but yielded a mean age of 17.0 ± 0.9 ka. We instead observe that the geomorphological position of the sample site, in particular with respect to the possibility to locally sustain remnant ice patches, is the stronger control on exposure ages. The correlation of age and elevation at individual sites presumably reflects that the ridges become narrower at higher elevations and can therefore sustain only thinner or no ice. This is particularly true at Dristner and Ahorn. In addition, during the Gschnitz stadial at 17–16 ka (Ivy-Ochs et al., 2006a) glaciers readvanced to a presumed terminal position at Mayrhofen (Penck and Brückner, 1901/1909). Lateral moraines on the hillslopes testify that ice margins were ~1000 m below our sample sites (Fig. 3A). Consequently, most of the 1500 m thick LGM ice must have disappeared before the Gschnitz stadial.

The influence of the geomorphological position of the study site is exemplified at Am Flach. As indicated by the name of the hillslope that translates to 'where it is flat', local topography is exceptionally smooth considering the altitude of 2140–2190 m. The ages of five boulder and bedrock samples are consistently around 15.2 ka, only ZA6 gives an age of 17.4 ± 1.0 ka. The Tettensjoch site is in the immediate vicinity, a ridge on the opposite side of the same hill at similar elevation (2090–2130 m), but steeper and narrower. Here the ages of four samples range from 18 to 16 ka. If by ~18 ka the LGM ice surface dropped sufficiently to expose the bedrock at Tettensjoch, it must have deposited the boulders at Am Flach simultaneously. In contrast to Tettensjoch, however, the flat high-elevation area at Am Flach has been conducive to the formation of local ice patches. The younger ages are therefore interpreted to reflect the melting of these remnant patches of ice that persisted on the flat landform and the associated complex exposure of the sampling sites.

Both ages at Ameiskopf are around 15 ± 1 ka. As the site is located further upvalley than the other locations, the position well inside the Gschnitz accumulation area potentially entails a greater susceptibility to ice cover during that period. It is conceivable that the slow rate of LGM ice decay kept the ice surface sufficiently high to cover the site until the Gschnitz stadial. In order to accomplish this, an ice thickness of 600 m in Zamsergrund would have to be sustained. Alternatively, a relatively thin ice cover on the Zamsergrund trough shoulder covering the samples would yield identical results (Wirsig et al., 2016).

5. Discussion

We first outline the implications from the combined dataset of the Mont Blanc and Zillertal Alps study sites concerning a) the potential influence of (glacial) erosion on the calculated exposure ages, b) synchronicity of ice surface lowering across the High Alps and c) temporary cover of the sample sites after the retreat of the LGM ice. Finally these results will be put into the context of an Alpine-wide and global deglaciation chronology.

5.1. Implications from both study areas

Rock surface erosion can potentially influence the measured nuclide concentrations in two ways: 1) insufficient erosion during the LGM would cause inheritance of pre-LGM nuclides and 2) post-LGM erosion would remove the rock surface with the highest nuclide concentration yielding too young ages (Ivy-Ochs et al., 2007). The lack of ages older than 18.5 ka in our data sets suggests that LGM glacial occupation was able to completely erode the pre-LGM ^{10}Be inheritance (Kelly et al., 2006; Wirsig et al., 2016). This shows that erosive, warm-based ice operated very close to the trimline (~30 m at the Gams site, Zillertal). To test our data sets for post-LGM erosion, we compare different sample types. Polished sample surfaces indicate negligible erosion since the disappearance of ice. Likewise, quartz veins are more resistant to weathering than the surrounding rock. If post-LGM erosion had a strong influence on our results, samples of these types would be expected to yield significantly older ages than the remaining samples. Indeed, three of the four oldest ages in the Zillertal Alps are from polished rock surfaces (ZA6,17,30). On the other hand, though, the surface of ZA1 with the absolutely oldest age was not polished. Furthermore, young ages of ~15 ka from other polished surfaces (ZA7,24,25) indicate that post-LGM erosion does not dominantly determine the exposure ages. We therefore conclude that differences in the ages of individual samples are caused by their different exposure histories, not by differences in pre-/or post-LGM erosion or loss of the sample surface.

First signs of ice surface lowering are registered at the Mont Blanc at 18.5 ± 1.1 ka, in Zillertal at 18.6 ± 1.4 ka. Considering the difference in location of the two study areas this level of agreement is quite remarkable. Today the Mont Blanc area in the Western Alps and the Zillertal in the Eastern Alps are subject to rather different climate regimes: while the Mont Blanc area is dominated by prevailing Westerlies, Zillertal is under a stronger continental influence. Today even on the regional level, the impact of higher temperature and lower precipitation to the south of Mont Blanc causes glaciers to be significantly smaller than to the north (Deline et al., 2012). From this perspective, synchronous lowering of the LGM ice surface in the two study regions could not have been assumed. During the LGM, however, a southward shift of the Polar Front caused dominating southerly atmospheric circulation for central Europe (Florineth and Schlüchter, 2000; Luetscher et al., 2015). Since the differences in precipitation and climate would have been smaller across the Alps during the LGM than they are today, synchronous behavior of the glacier systems in east and west was more likely. Nevertheless, the uncertainties of the dating approach leave room for undetected asynchrony.

The oldest ages in this study of ~18.5 ka were only determined at few sample locations, however. In contrast, most of the remaining boulders and bedrock surfaces, 23 of 32 samples, were exposed for 16.4–14.8 ka. Since the unexpectedly young ages were not caused by erosion, we propose that local patches of ice persisted for part of the Lateglacial at high altitudes in both study areas. In the proximity of the Zillertal Alps the Gschnitz ELA has been estimated to be at 1860–1950 m (Gross et al., 1977; Kerschner et al., 1999; Zasadni, 2014). According to this, most (20 of 22) Zillertal Alps samples are from the Gschnitz accumulation zone where the build-up of local ice patches is plausible, if allowed by topography. The same is valid for the samples in the Mont Blanc study area due to their location at high elevations. Temperatures in the Alps were considerably colder than today until the Bølling-Allerød interstadial, e.g. summers were 8–10° colder during Gschnitz (Kerschner, 2009; Schmidt et al., 2009), which enabled the accumulation of local patches of ice that persisted at high altitudes for at least part of the Lateglacial if topography allowed. This has been proposed in particular at concave settings such as High Alpine passes or trough shoulders (Ivy-Ochs et al., 2006b; Böhlert et al., 2011; Hippe et al., 2014; Wirsig et al., 2016). Considering the culmination of evidence, it can be stated tentatively that the phenomenon of ice patches persisting after the LGM at high elevations might have occurred across the Alps. Consistent minimum exposure ages of ~15 ka at all sites indicate that the ice patches disappeared before or at the onset of the Bølling-Allerød interstadial.

5.2. The deglaciation chronology of the High Alps in context

The best chronological constraint on the LGM fluctuations in the

foreland lobes in the Alps is from the Tagliamento amphitheater (Fig. 5; Monegato et al., 2007; Fontana et al., 2014). The first Tagliamento glacial pulse – the Santa Margherita phase - occurred between 26.5 and 23 ka. The glacier readvanced within the amphitheater between 23 and 21 ka during the Canodusso phase and it remained there through the Remanzacco recessional phase that ended at 19 ka (Monegato et al., 2007). A culmination of evidence that emerged during the last decade (Fig. 5) demonstrates that many foreland lobes reached their maximum position before 23–22 ka, thus during Greenland Stadial 3 (Rasmussen et al., 2014) or the global LGM as proposed by Hughes and Gibbard (2015). An early advance, which would correlate to the Santa Margherita phase of the Tagliamento Glacier (26.5–23 ka), has also been dated in other Italian morainic amphitheaters (e.g. Ravazzi et al., 2012; Scapozza et al., 2015). This advance could have its equivalent in the Maritime Alps in the Durance Valley (Jorda et al., 2000) and the Gesso Glacier (Federici et al., 2012, 2016). Similarly, in the northern Swiss foreland, exposure ages pinpoint the initiation of withdrawal from the maximum positions at 24 ± 2 ka at the Rhône glacier (Ivy-Ochs et al., 2004) and at 22 ± 2 ka at the Reuss glacier (Reber et al., 2014; Ivy-Ochs, 2015). The presented exposure ages from the trimlines at Mont Blanc and in the Zillertal Alps show that the lowering of the ice surface was certainly delayed with respect to the abandonment of the maximum positions of piedmont glaciers at many places around the Alps at 26–22 ka (Fig. 5).

Numerous chronological constraints on the fluctuation of the foreland lobes suggest abandonment of the maximum positions or recessional stages which overlap in time with the Remanzacco phase (>19 ka, Monegato et al., 2007): 18.6–17.9 ka for the Oglio Glacier in the Iseo amphitheater (Ravazzi et al., 2012); 19.8–17.6 ka for the Traun Glacier (van Husen, 1997) and 19.7 ± 1.4 ka for the Isar-Loisach Glacier (Reuther et al., 2011); in the northwest 18.6 ± 0.9 ka for the Reuss Glacier (Reber et al., 2014) and 18 ± 1 ka for the Linth-Rhein Glacier (Lister, 1988). Initial lowering of the ice surface in the High Alps therefore appears to have occurred broadly synchronous (within the resolution of the dating method) to marked retreat of the piedmont lobes and ice-free forelands soon after 19 ka (van Husen, 1987; Lister, 1988; Schlüchter and Röthlisberger, 1995; Monegato et al., 2007; Reitner, 2007; Lauterbach et al., 2012; Schmidt et al., 2012; Baroni et al., 2014; Ravazzi et al., 2014).

Delayed ice surface lowering in the High Alps with respect to the initial retreat from the maximum position of glacier lobes in the forelands (26–22 ka) can be explained by its location in the upper reaches of the glacier systems, more than 100 km from the piedmont lobe termini. In those settings a smaller and mitigated change of ice surface elevation in reaction to the fluctuation in the glacier terminal zones is reasonable. Because our samples are not located directly at the trimline there could have been undetected initial lowering of ice surface elevation before 18.5 ka. The oldest ages obtained in the Mont Blanc area (Cou3) and in the Zillertal Alps (ZA1,6,17,30) are located 90 and on average 120 m below the trimline, respectively. Assuming that the glacial trimline in the Alps represents the subaerial to subglacial boundary, this means that these locations were exposed for the first time when glaciers had lost about 10% of their maximal thickness in the valleys which was

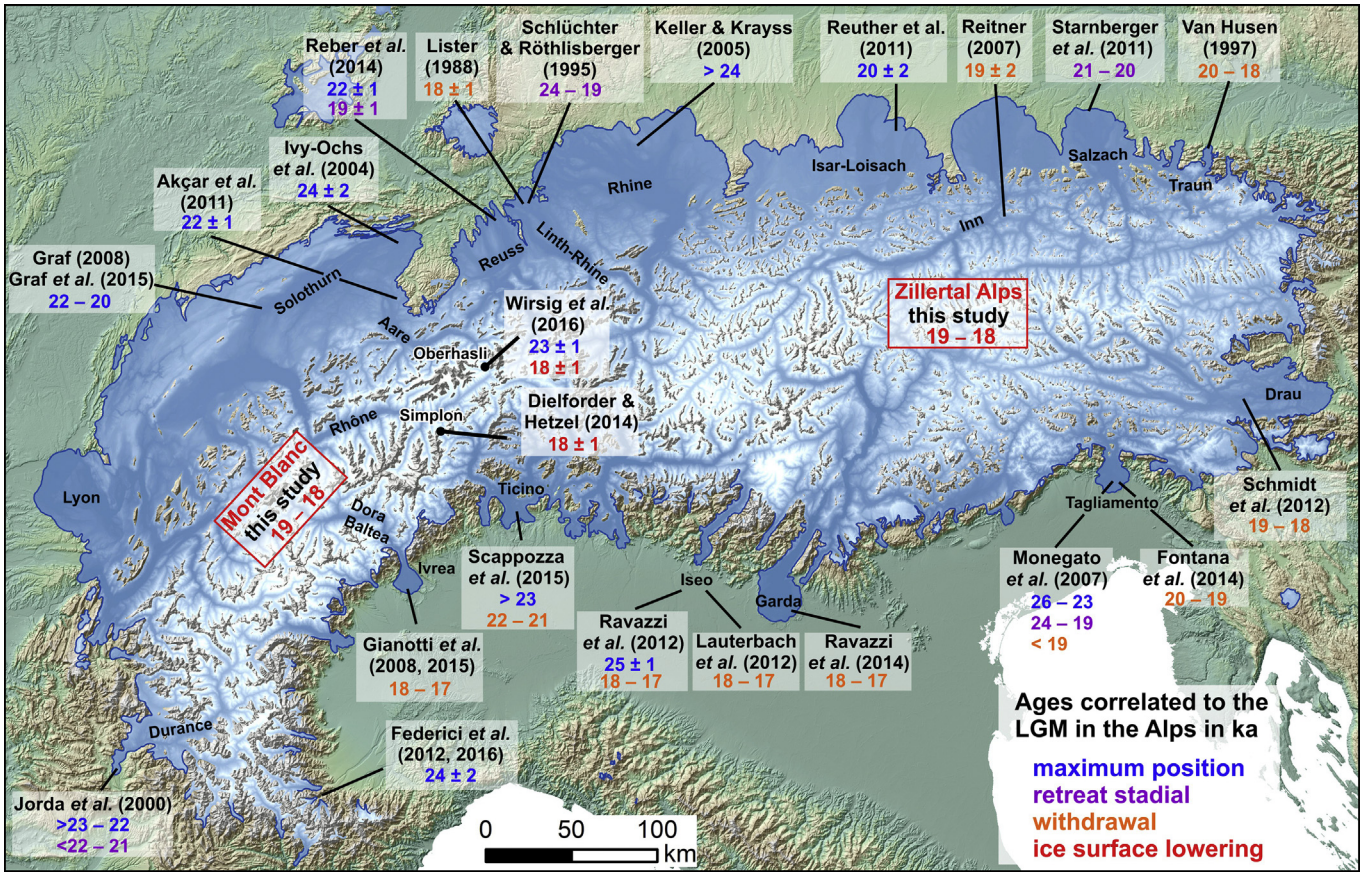

Fig. 5. Ages correlated to the LGM in the Alps. The map shows the results of this study in the context of a compilation of published ages by Ivy-Ochs (2015) that were correlated to the end of the LGM in the Alps. The type color indicates in which context an age has been interpreted by the authors. The LGM ice extent is from Ehlers and Gibbard (2004, http://www.qpg.geog.cam.ac.uk/lgmextent.html, accessed 20.11.2015).

~1000 m (Fig. 3). As shown by Wirsig et al. (2016), exposure ages from a high elevation trimline site in the central Swiss Alps can record stepwise lowering after full LGM conditions with the first sign of ice surface lowering about 50 m at 23 ± 0.8 ka, tentatively linked to the initial foreland glacier retreat after reaching of the maximum LGM positions. However, more evidence in other locations in the Alps is needed to confirm this hypothesis.

It cannot however be excluded that some portion of the terrain above the trimline was covered by cold-based, non-erosive ice and that the trimline in the Alps represents an englacial thermal boundary. Nevertheless, this hypothesis would be hard to prove or disprove in the Alps using exposure ages. For example, in the British Isles the blockfield-mantled summit plateaus are clearly distinguishable morphologically from the glacially eroded ice-stream valley slopes (Ballantyne, 1997; Ballantyne and Stone, 2015). The periglacial zone in the Alps is completely different; the zone above the glacial trimline comprises sharp arêtes and steep rock walls. Deposition and/or preservation of datable erratic boulders is therefore unlikely. Dating the bedrock surfaces above the trimline has been attempted previously in the Alps: Böhlert et al. (2008) presented ages ranging from 40 to 2 ka from steep rock walls and arêtes located far above the LGM ice surface in the Mont Blanc area. This showed that in both cases (subaerial to subglacial boundary and englacial thermal boundary) one could equally obtain pre-LGM, LGM and post-LGM ages.

Whether or not there was an englacial thermal boundary, retreat of the glacier lobes after 19 ka in the foreland and the onset of loss of the major part of ice in the High Alps at 18.5 ka occurred nearly synchronously. This implies prominent reorganization of Alpine ice cover from vast 100–300 km long transection glaciers supplying the foreland glacier lobes (van Husen, 1987; Bini et al., 2009) to one order of magnitude shorter local mountain glaciers during the Gschnitz stadial advance (van Husen, 1997; Ivy-Ochs et al., 2006a; Ivy-Ochs, 2015). Therefore, most of the LGM ice volume in the High Alps must have disappeared before 17–16 ka, because at this time Gschnitz glaciers advanced into ice-free terrain (Ivy-Ochs et al., 2008). This left very little time, ca. 1–2 ka, for complete deglaciation of 1000–1500 m of LGM ice in the High Alpine valleys and implies rapid ice surface lowering rates (Schlüchter, 1988).

The onset of ice surface lowering in the High Alps is potentially synchronous to the Längsee warm oscillation at 18.5–18.1 ka that preceded the return of severe climate cooling during Heinrich 1 event and the Gschnitz stadial glacier advances (Schmidt et al., 2012). This warming triggered a glacier mass balance change above a critical threshold that no longer allowed support of the full LGM glacial geometry condition in the Alps (Reitner, 2007). This crisis could also be amplified with precipitation starving associated with cessation of the southward shifted trajectory of North Atlantic storm track in the Alps at 19 ka recorded in Sieben Hengste speleothems (Luetscher et al., 2015). The onset of ice surface lowering in the Alps is associated with accelerated retreat of glaciers in mid latitudes at 19–18 ka (Schaefer et al., 2006; Clark et al., 2009), where a globally increased rate of deglaciation after full LGM conditions contributed to the 19 ka meltwater pulse (Lambeck et al., 2000, 2014). Across the Eurasian Ice Sheet the timing of advance and retreat were remarkably spatially variable. However, the peak in its total area and volume occurred at 21–20 ka and initial retreat occurred soon after 19 ka (Hughes et al., 2016b and references therein). Similar conclusions can be drawn from the LGM evolution of the British-Irish component of this ice sheet, which at 19 ka was in crisis with considerable ice loss and dynamic thinning (Clark et al., 2012). Exposure ages located in the center zone of the LGM Welsh Ice Cap show rapid thinning after the LGM at 19 ± 1 ka and exposure of summits in North Wales as nunataks (Hughes et al., 2016a). The presented results strengthen the evidence of remarkable climatic change and glacier reaction in the mid-latitudes at 19–18 ka that was not seen in isotopic records from high latitude Greenland ice cores (Schaefer et al., 2006).

6. Conclusions

The oldest exposure ages from bedrock and erratic boulder surfaces from high elevation ridges just beneath the glacial trimline in the High Alps are 18.5 ± 1.1 ka in the Mont Blanc area (Western Alps) and 18.6 ± 1.4 ka in the Zillertal Alps (Eastern Alps). They indicate that the ice surface in the High Alps likely remained close to its maximum elevation throughout full LGM conditions when glacier tongues fluctuated on the Alpine forelands (26.5–19 ka). Trimline positions were finally abandoned synchronous with significant retreat of the piedmont lobes soon after 19 ka, presumably during the Längsee warm oscillation (18.5–18.1 ka). Identical ages from both study areas, as well a similar results obtained in the Swiss Alps (Dielforder and Hetzel, 2014; Wirsig et al., 2016) suggest synchronous initiation of LGM ice surface lowering in the accumulation zones of transection glacier systems across the Alps. Decline of Alpine ice cover during the early Lateglacial was extremely rapid; most of the ice in the LGM accumulation centers must have disappeared in a short time (~1–2 ka) before local Gschnitz valley glaciers started to advance into ice-free terrain in response to Heinrich 1 stadial conditions (17–15.4 ka).

The simultaneous ice-surface lowering and complete abandonment of the forelands by the piedmont lobes soon after 19 ka was likely amplified by moisture starvation due to northward shift of the North Atlantic storm track at 19 ka (Luetscher et al., 2015).

Acknowledgements

This work was funded by the Swiss National Fonds (SNF), project 2-77099-11 to S. Ivy-Ochs and by AGH-UST statutory grant No. 15.11.140.626 to J. Zasadni. All members of the Laboratory of Ion Beam Physics group at ETH are recognized for their commitment and support of this project. Special thanks go to A. Madella and C. Spötl for help during fieldwork.

References

Akcar, N., Ivy-Ochs, S., Kubik, P., Schlüchter, C., 2011. Post-depositional impacts on 'Findlinge' (erratic boulders) and their implications for surface-exposure dating. Swiss J. Geosciences 104, 445–453. http://dx.doi.org/10.1007/s00015-011-0088-7.

Balco, G., Stone, J.O., Lifton, N.A., Dunai, T.J., 2008. A complete and easily accessible means of calculating surface exposure ages or erosion rates from ^{10}Be and ^{26}Al measurements. Quat. Geochronol. 3, 174–195. http://dx.doi.org/10.1016/j.quageo.2007.12.001.

Balco, G., Briner, J., Finkel, R.C., Rayburn, J.A., Ridge, J.C., Schaefer, J.M., 2009. Regional beryllium-10 production rate calibration for late-glacial northeastern North America. Quat. Geochronol. 4, 93–107. http://dx.doi.org/10.1016/j.quageo.2008.09.001.

Ballantyne, C.K., 1997. Periglacial trimline in the scottish highlands. Quat. Int. 38/39, 119–136. http://dx.doi.org/10.1016/S1040-6182(96)00016-X.

Ballantyne, C.K., Stone, J.O., 2015. Trimlines, blockfields and the vertical extent of the last ice sheet in southern Ireland. Boreas 44, 277–287. http://dx.doi.org/10.1111/bor.12109.

Baroni, C., Martino, S., Salvatore, M.C., Mugnozza, G.S., Schilirò, L., 2014. Thermo-mechanical stress–strain numerical modelling of deglaciation since the last glacial maximum in the adamello group (rhaetian Alps, Italy). Geomorphology 226, 278–299. http://dx.doi.org/10.1016/j.geomorph.2014.08.013.

Bierman, P.R., Caffee, M.W., Davis, P.T., Marsella, K., Pavich, M., Colgan, P., Mickelson, D., Larsen, J., 2002. Rates and timing of earth surface processes from in situ-produced cosmogenic Be-10. Rev. Mineralogy Geochem. 50, 147–205. http://dx.doi.org/10.2138/rmg.2002.50.4.

Bini, A., Buoncristiani, J.F., Couterrand, S., Ellwanger, D., Felber, M., Florineth, D., Graf, H.R., Keller, O., Kelly, M., Schlüchter, C., Schoeneich, P., 2009. Switzerland during the Last Glacial Maximum 1: 500,000. Bundesamt für Landestopografie swisstopo.

Bobek, H., 1932. Alte Gletscherstände im Gebiet der Zillertaler und Tuxer Alpen.

Z. für Gletscherkd. 20, 138–158.
Bobek, H., 1933. Die Formenentwicklung der Zillertaler und Tuxer Alpen im Einzugsbereich des Zillers. Forschungen zur Dtsch. Landes- Volkskd. 30.
Böhlert, R., Egli, M., Maisch, M., Brandová, D., Ivy-Ochs, S., Kubik, P.W., Haeberli, W., 2011. Application of a combination of dating techniques to reconstruct the Lateglacial and early Holocene landscape history of the Albula region (eastern Switzerland). Geomorphology 127, 1–13. http://dx.doi.org/10.1016/j.geomorph.2010.10.034.
Böhlert, R., Gruber, S., Egli, M., Maisch, M., Brandova, D., Haeberli, W., Ivy-Ochs, S., Christl, M., Kubik, P.W., Deline, P., 2008. Comparison of exposure ages and spectral properties of rock surfaces in steep, high alpine rock walls of Aiguille du Midi, France. In: 9th International Conference on Permafrost, Fairbanks, Alaska, 29 June 2008-03 July 2008, pp. 143–148.
Chaline, J., Jerz, H., 1984. Arbeitsergebnisse der Subkommission für Europäische Quartärstratigraphie Stratotypen des Würmglazials (Berichte der SEQS 6). Eiszeitalt. Ggw. 35, 185–206.
Christl, M., Vockenhuber, C., Kubik, P.W., Wacker, L., Lachner, J., Alfimov, V., Synal, H.A., 2013. The ETH Zurich AMS facilities: performance parameters and reference materials. Nucl. Instrum. Methods Phys. Res. Sect. B Beam Interact. Mater. Atoms 294, 29–38. http://dx.doi.org/10.1016/j.nimb.2012.03.004.
Clark, P.U., Dyke, A.S., Shakun, J.D., Carlson, A.E., Clark, J., Wohlfarth, B., Mitrovica, J.X., Hostetler, S.W., McCabe, A.M., 2009. The last glacial maximum. Science 325, 710–714. http://dx.doi.org/10.1126/science.1172873.
Clark, C.D., Hughes, A.L.C., Greenwood, S.L., Jordan, C., Sejrup, H.P., 2012. Pattern and timing of retreat of the last british-irish ice sheet. Quat. Sci. Rev. 44, 112–146. http://dx.doi.org/10.1016/j.quascirev.2010.07.019.
Cossart, E., Fort, M., Bourlès, D., Braucher, R., Perrier, R., Siame, L., 2012. Deglaciation pattern during the Lateglacial/Holocene transition in the southern French Alps. Chronological data and geographical reconstruction from the Clarée Valley (upper Durance catchment, southeastern France). Palaeogeogr. Palaeoclimatol. Palaeoecol. 315–316, 109–123. http://dx.doi.org/10.1016/j.palaeo.2011.11.017.
Coutterand, S., Buoncristiani, J., 2006. Paléogéographie du dernier maximum glaciaire du pléistocène récent de la région du masif du Mont Blanc, France. Quaternaire 17, 35–43. http://dx.doi.org/10.4000/quaternaire.633.
de Saussure, H.B., 1779–1796. Voyages dans les Alpes (Fauche, Genéve).
Deline, P., Gardent, M., Magnin, F., Ravanel, L., 2012. The morphodynamics of the Mont Blanc massif in a changing cryosphere: a comprehensive review. Geografiska Annaler: series A. Phys. Geogr. 94, 265–283. http://dx.doi.org/10.1111/j.1468-0459.2012.00467.x.
Delunel, R., Bourlés, D.L., van der Beek, P.A., Schlunegger, F., Leya, I., Masarik, J., Paquet, E., 2014. Snow shielding factors for cosmogenic nuclide dating inferred from long-term neutron detector monitoring. Quat. Geochronol. 24, 16–26. http://dx.doi.org/10.1016/j.quageo.2014.07.003.
Dielforder, A., Hetzel, R., 2014. The deglaciation history of the Simplon region (southern Swiss Alps) constrained by ^{10}Be exposure dating of ice-molded bedrock surfaces. Quat. Sci. Rev. 84, 26–38. http://dx.doi.org/10.1016/j.quascirev.2013.11.008.
Dunai, T.J., Binnie, S.A., Hein, A.S., Paling, S.M., 2014. The effects of a hydrogen-rich ground cover on cosmogenic thermal neutrons: implications for exposure dating. Quat. Geochronol. 22, 183–191. http://dx.doi.org/10.1016/j.quageo.2013.01.001.
Ehlers, J., Gibbard, P.L., 2004. Quaternary Glaciations-extent and Chronology: Part I: Europe. Elsevier.
Evans, I.S., 2006. Glacier distribution in the Alps: statistical modelling of altitude and aspect. Geografiska Annaler. Series A. Phys. Geogr. 88, 115–133. http://dx.doi.org/10.1111/j.0435-3676.2006.00289.x.
Fabel, D., Stroeven, A.P., Harbor, J., Kleman, J., Elmore, D., Fink, D., 2002. Landscape preservation under Fennoscandian ice sheets determined from in situ produced ^{10}Be and ^{26}Al. Earth Planet. Sci. Lett. 201, 397–406. http://dx.doi.org/10.1016/S0012-821X(02)00714-8.
Federici, P.R., Granger, D.E., Ribolini, A., Spagnolo, M., Pappalardo, M., Cyr, A.J., 2012. Last glacial maximum and the Gschnitz stadial in the maritime Alps according to ^{10}Be cosmogenic dating. Boreas 41, 277–291. http://dx.doi.org/10.1111/j.1502-3885.2011.00233.x.
Federici, P.R., Ribolini, A., Spagnolo, M., 2016. T glacial history of the maritime Alps from the last glacial maximum to the little ice age. Geol. Soc. Lond. Spec. Publ. 433, SP433–SP439. http://dx.doi.org/10.1144/SP433.9.
Florineth, D., 1998. Surface geometry of the Last Glacial Maximum (LGM) in the southeastern Swiss Alps (Graubünden) and its paleoclimatological significance. Eiszeitalt. Ggw. 48, 23–37.
Florineth, D., Schlüchter, C., 1998. Reconstructing the last glacial maximum (LGM) ice surface geometry and flowlines in the central Swiss Alps. Eclogae Geol. Helvetiae 91, 391–407.
Florineth, D., Schlüchter, C., 2000. Alpine evidence for atmospheric circulation patterns in Europe during the last glacial maximum. Quat. Res. 54, 295–308. http://dx.doi.org/10.1006/qres.2000.2169.
Fohlmeister, J., Vollweiler, N., Spötl, C., Mangini, A., 2013. COMNISPA II: update of a mid-European isotope climate record, 11 ka to present. Holocene 23, 749–754. http://dx.doi.org/10.1177/0959683612465446.
Fontana, A., Monegato, G., Zavagno, E., Devoto, S., Burla, I., Cucchi, F., 2014. Evolution of an alpine fluvioglacial system at the LGM decay: the cormor megafan (NE Italy). Geomorphology 204, 136–153. http://dx.doi.org/10.1016/j.geomorph.2013.07.034.
Frisch, W., 1980. Tectonics of the western tauern window. Mittl. Österreichischen Geol. Ges. 71, 65–71.
Froitzheim, N., Plašienka, D., Schuster, R., 2008. Alpine tectonics of the Alps and western carpathians. In: The Geology of Central Europe. The Geological Society of London, pp. 1141–1232.
Gianotti, F., Forno, M.G., Ivy-Ochs, S., Kubik, P., 2008. New chronological and stratigaphical data on the Ivrea amphitheatre (Piedmont, NW Italy). Quat. Int. 190, 123–135. http://dx.doi.org/10.1016/j.quaint.2008.03.001.
Gianotti, F., Forno, M.G., Ivy-Ochs, S., Monegato, G., Pini, R., Ravazzi, C., 2015. Stratigraphy of the Ivrea morainic amphitheatre (NW Italy): an updated synthesis. Alp. Mediterr. Quat. 28, 29–58.
Gosse, J.C., Phillips, F.M., 2001. Terrestrial in situ cosmogenic nuclides: theory and application. Quat. Sci. Rev. 20, 1475–1560. http://dx.doi.org/10.1016/S0277-3791(00)00171-2.
Graf, A.A., 2008. Surface Exposure Dating on LGM and pre-LGM Erratic Boulders – A Comparison of Paleoclimate Records from both Hemispheres (PhD thesis). University of Bern, Bern, Switzerland.
Graf, A., Akçar, N., Ivy-Ochs, S., Strasky, S., Kubik, P.W., Christl, M., Burkhard, M., Wieler, R., Schlüchter, C., 2015. Multiple advances of alpine glaciers into the jura mountains in the northwestern Switzerland. Swiss J. Geosciences 1–14. http://dx.doi.org/10.1007/s00015-015-0195-y.
Gross, G., Kerschner, H., Patzelt, G., 1977. Methodische Untersuchungen über die Schneegrenze in alpinen Gletschergebieten. Z. für Gletscherkd. Glazialgeol. 12, 223–251.
Hättestrand, C., Stroeven, A.P., 2002. A relict landscape in the centre of Fennoscandian glaciation: geomorphological evidence of minimal Quaternary glacial erosion. Geomorphology 44, 127–143. http://dx.doi.org/10.1016/S0169-555X(01)00149-0.
Heuberger, H., 1968. Geomorphologische beschreibung. In: Trogtal, Alpines, Zillertal, Gunggl im (Eds.), Landformen im Kartenbild - Gruppe V: Zentralalpen, Kartenprobe 2, pp. 6–11. Westermann.
Heuberger, H., 1977. Gletscher- und klimageschichtliche Untersuchungen im Zemmgrund. Alpenvereinsjahrbuch 102, 39–50.
Hippe, K., Ivy-Ochs, S., Kober, F., Zasadni, J., Wieler, R., Wacker, L., Kubik, P.W., Schlüchter, C., 2014. Chronology of Lateglacial ice flow reorganization and deglaciation in the Gotthard Pass area, Central Swiss Alps, based on cosmogenic ^{10}Be and in situ ^{14}C. Quat. Geochronol. 19, 14–26. http://dx.doi.org/10.1016/j.quageo.2013.03.003.
Hoelzle, M., 1996. Mapping and modelling of mountain permafrost distribution in the Alps. Norsk Geografisk Tidsskrift-Norwegian J. Geogr. 50, 11–15. http://dx.doi.org/10.1080/00291959608552347.
Hughes, P.D., Gibbard, P.L., 2015. A stratigraphical basis for the last glacial maximum (LGM). Quat. Int. 383, 174–185. http://dx.doi.org/10.1016/j.quaint.2014.06.006.
Hughes, P.D., Glasser, N.F., Fink, D., 2016a. Rapid thinning of the Welsh Ice Cap at 20-19 ka based on 10Be ages. Quat. Res. 85, 107–117. http://dx.doi.org/10.1016/j.yqres.2015.11.003.
Hughes, A.L.C., Gyllencreutz, R., Lohne, Ø.S., Mangerud, J., Svendsen, J.I., 2016b. The last Eurasian ice sheets – a chronological database and time-slice reconstruction, DATED-1. Boreas 45, 1–45. http://dx.doi.org/10.1111/bor.12142.
Ivy-Ochs, S., 1996. The Dating of Rock Surfaces Using in Situ Produced ^{10}Be, ^{26}Al and ^{36}Cl, with Examples from Antarctica and the Swiss Alps (PhD thesis). ETH, Zürich.
Ivy-Ochs, S., Schaefer, J., Kubik, P., Synal, H.A., Schlüchter, C., 2004. Timing of deglaciation on the northern Alpine foreland (Switzerland). Eclogae Geol. Helvetiae 97, 47–55.
Ivy-Ochs, S., Kerschner, H., Kubik, P.W., Schlüchter, C., 2006a. Glacier response in the european Alps to Heinrich event 1 cooling: the Gschnitz stadial. J. Quat. Sci. 21, 115–130. http://dx.doi.org/10.1002/jqs.955.
Ivy-Ochs, S., Kerschner, H., Reuther, A., Maisch, M., Sailer, R., Schaefer, J., Kubik, P.W., Synal, H.A., Schlüchter, C., 2006b. The timing of glacier advances in the northern European Alps based on surface exposure dating with cosmogenic ^{10}Be, ^{26}Al, ^{36}Cl and ^{21}Ne. Geol. Soc. Am. Special Pap. 415, 43–60. http://dx.doi.org/10.1130/2006.2415(04).
Ivy-Ochs, S., Kerschner, H., Schlüchter, C., 2007. Cosmogenic nuclides and the dating of Lateglacial and Early Holocene glacier variations: the Alpine perspective. Quat. Int. 164–165, 53–63. http://dx.doi.org/10.1016/j.quaint.2006.12.008.
Ivy-Ochs, S., Kober, F., 2008. Surface exposure dating with cosmogenic nuclides. Quat. Sci. J. 57, 179–209.
Ivy-Ochs, S., Kerschner, H., Reuther, A., Preusser, F., Heine, K., Maisch, M., Kubik, P.W., Schlüchter, C., 2008. Chronology of the last glacial cycle in the European Alps. J. Quat. Sci. 23, 559–573. http://dx.doi.org/10.1002/jqs.1202.
Ivy-Ochs, S., Briner, J., 2014. Dating disappearing ice with cosmogenic nuclides. J. Elem. 10, 341–346. http://dx.doi.org/10.2113/gselements.10.5.351.
Ivy-Ochs, S., 2015. Glacier variations in the European Alps at the end of the last glaciation. Cuad. Investig. Geográfica 41, 295–315.
Jäckli, H., 1962. Die Vergletscherung der Schweiz im Würmmaximum. Eclogae Geol. Helvetiae 55, 285–294.
Jorda, M., Rosique, T., Évinc, J., 2000. Données nouvelles sur l'âge du dernier maximum glaciaire dans les Alpes méridionales françaises. Earth Planet. Sci. 331, 187–193.
Keller, O., Krayss, E., 2005. Der Rhein-Linth-Gletscher im letzten Hochglazial, 2. Teil: Datierung und Modelle der Rhein-Linth-Vergletscherung. Klima-Rekonstruktionen. Vierteljahresschrift der Naturforschenden Gesellschaft Zürich 150, 69–85.
Kelly, M., Buoncristiani, J.F., Schlüchter, C., 2004. A reconstruction of the last glacial maximum (LGM) ice-surface geometry in the western Swiss Alps and contiguous Alpine regions in Italy and France. Eclogae Geol. Helvetiae 97, 57–75.

Kelly, M.A., Ivy-Ochs, S., Kubik, P., von Blanckenburg, F., Schlüchter, C., 2006. Chronology of deglaciation based on ^{10}Be dates of glacial erosional features in the Grimsel Pass region, central Swiss Alps. Boreas 35, 634–643. http://dx.doi.org/10.1080/03009480600690829.

Kerschner, H., 1986. Zum Sendersstadium im Spätglazial der nördlichen Stubaier Alpen, Tirol. Z. für Geomorphol. 61, 65–76.

Kerschner, H., Ivy-Ochs, S., Schlüchter, C., 1999. Paleoclimatic interpretation of the early Late-glacial glacier in the Gschnitz valley, central Alps, Austria. Ann. Glaciol. 28, 135–140. http://dx.doi.org/10.3189/172756499781821661.

Kerschner, H., 2009. Gletscher und Klima im Alpinen Spätglazial und frühen Holozän. Innsbruck University Press.

Klasen, N., Fiebig, M., Preusser, F., Reitner, J.M., Radtke, U., 2007. Luminescence dating of proglacial sediments from the Eastern Alps. Quat. Int. 164–165, 21–32. http://dx.doi.org/10.1016/j.quaint.2006.12.003.

Kohl, C.P., Nishiizumi, K., 1992. Chemical isolation of quartz for measurement of in-situ -produced cosmogenic nuclides. Geochimica Cosmochimica Acta 56, 3583–3587.

Lambeck, K., Yokoyama, Y., Johnston, P., Purcell, A., 2000. Global ice volumes at the last glacial maximum and early lateglacial. Earth Planet. Sci. Lett. 181, 513–527. http://dx.doi.org/10.1016/S0012-821X(00)00223-5.

Lambeck, K., Rouby, H., Purcell, A., Sun, Y., Sambridge, M., 2014. Sea level and global ice volumes from the last glacial maximum to the Holocene. Proc. Natl. Acad. Sci. 111, 15296–15303. http://dx.doi.org/10.1073/pnas.1411762111.

DecLakes Participants Lauterbach, S., Chapron, E., Brauer, A., Hüls, M., Gilli, A., Arnaud, F., Piccin, A., Nomade, J., Desmet, M., von Grafenstein, U., 2012. A sedimentary record of Holocene surface runoff events and earthquake activity from Lake Iseo (Southern Alps, Italy). Holocene 22, 749–760. http://dx.doi.org/10.1177/0959683611430340.

Lister, G.S., 1988. A 15,000-year isotopic record from Lake Zürich of deglaciation and climatic change in Switzerland. Quat. Res. 29, 129–141. http://dx.doi.org/10.1016/0033-5894(88)90056-7.

Louis, H., Fischer, K., 1979. Allgemeine Geomorphologie. de Gruyter.

Luetscher, M., Boch, R., Sodemann, H., Spötl, C., Cheng, H., Edwards, R., Frisia, S., Hof, F., Müller, W., 2015. North Atlantic storm track changes during the last glacial maximum recorded by alpine speleothems. Nat. Commun. 6, 1–6. http://dx.doi.org/10.1038/ncomms7344.

Mayr, F., Heuberger, H., 1968. Type areas of lateglacial and postglacial deposits in tyrol, eastern Alps. Proceeding VII INQUA Congr. 14, 143–165.

Monegato, G., Ravazzi, C., Donegana, M., Pini, R., Calderoni, G., Wick, L., 2007. Evidence of a two-fold glacial advance during the last glacial maximum in the Tagliamento end moraine system (eastern Alps). Quat. Res. 68, 284–302. http://dx.doi.org/10.1016/j.yqres.2007.07.002.

Nishiizumi, K., Imamura, M., Caffee, M.W., Southon, J.R., Finkel, R.C., McAninch, J., 2007. Absolute calibration of ^{10}Be AMS standards. Nucl. Instrum. Methods Phys. Res. Sect. B Beam Interact. Mater. Atoms 258, 403–413. http://dx.doi.org/10.1016/j.nimb.2007.01.297.

Penck, A., Brückner, E., 1901/1909. Die Alpen im Eiszeitalter. Tauchitz, Leipzig.

Penck, A., 1905. Glacial features in the surface of the Alps. J. Geol. 13, 1–19.

Pfiffner, O.A., 2014. Geology of the Alps. John Wiley & Sons.

Porter, S., Orombelli, G., 1982. Late-glacial ice advances in the western Italian Alps. Boreas 11, 125–140. http://dx.doi.org/10.1111/j.1502-3885.1982.tb00530.x.

Rasmussen, S.O., Bigler, M., Blockley, S.P., Blunier, T., Buchardt, S.L., Clausen, H.B., Cvijanovic, I., Dahl-Jensen, D., Johnsena, S.J., Fischer, H., Gkinis, V., Guillevic, M., Hoek, W.Z., Lowe, J.J., Pedro, J.B., Popp, T., Seierstad, I.K., Steffensen, J.P., Svensson, A.M., Vallelonga, P., Vinther, B.M., Walker, M.J.C., Wheatley, J.J., Winstrup, M., 2014. A stratigraphic framework for abrupt climatic changes during the Last Glacial period based on three synchronized Greenland ice-core records: refining and extending the INTIMATE event stratigraphy. Quat. Sci. Rev. 106, 14–28. http://dx.doi.org/10.1016/j.quascirev.2014.09.007.

Ravazzi, C., Badino, F., Marsetti, D., Patera, G., Reimer, P.J., 2012. Glacial to paraglacial history and forest recovery in the Oglio glacier system (Italian Alps) between 26 and 15 ka cal BP. Quat. Sci. Rev. 58, 146–161. http://dx.doi.org/10.1016/j.quascirev.2012.10.017.

Ravazzi, C., Pini, R., Badino, F., De Amicis, M., Londeix, L., Reimer, P.J., 2014. The latest LGM culmination of the Garda Glacier (Italian Alps) and the onset of glacial termination. Age of glacial collapse and vegetation chronosequence. Quat. Sci. Rev. 105, 26–47. http://dx.doi.org/10.1016/j.quascirev.2014.09.014.

Reber, R., Akcar, N., Ivy-Ochs, S., Tikhomirov, D., Burkhalter, R., Zahno, C., Lüthold, A., Kubik, P.W., Vockenhuber, C., Schlüchter, C., 2014. Timing of retreat of the Reuss glacier (Switzerland) at the end of the last glacial maximum. Swiss J. Geosciences 1–15. http://dx.doi.org/10.1007/s00015-014-0169-5.

Reitner, J., 2007. Glacial dynamics at the beginning of Termination I in the Eastern Alps and their stratigraphic implications. Quat. Int. 164–165, 64–84. http://dx.doi.org/10.1016/j.quaint.2006.12.016.

Reitner, J., 2013. The Effect of Climate Change during the Lateglacial in the Hohen Tauern. 5th Symposium for Research in Protected Areas, pp. 653–658.

Reuther, A., Fiebig, M., Ivy-Ochs, S., Kubik, P., Reitner, J., Jerz, H., Heine, K., 2011. Deglaciation of a large piedmont lobe glacier in comparison with a small mountain glacier – new insight from surface exposure dating. Two studies from SE Germany. Quat. Sci. J. 60, 248–269.

Scapozza, C., Castelletti, C., Soma, L., Dall'Agnolo, S., Ambrosi, C., 2015. Timing of LGM and deglaciation in the southern Swiss Alps. Géomorphologie 4, 307–322.

Schaefer, J.M., Denton, G.H., Barrell, D.J.A., Ivy-Ochs, S., Kubik, P.W., Andersen, B.G., Phillips, F.M., Lowell, T.V., Schlüchter, C., 2006. Near-synchronous interhemispheric termination of the last glacial maximum in mid-latitudes. Science 312, 1510–1513. http://dx.doi.org/10.1126/science.1122872.

Schildgen, T.F., Phillips, W.M., Purves, R.S., 2005. Simulation of snow shielding corrections for cosmogenic nuclide surface exposure studies. Geomorphology 64, 67–85. http://dx.doi.org/10.1016/j.geomorph.2004.05.003.

Schlüchter, C., 1988. The deglaciation of the Swiss Alps: a palaeoclimatic event with chronological problems. Bull. l'Association Francaise l'Etude Quat. 25, 141–145.

Schlüchter, C., Röthlisberger, C., 1995. 100,000 jahre gletschergeschichte. In: Gletscher im ständigen Wandel, pp. 47–63 vdf-Verlag: Zürich.

Schmidt, R., Drescher-Schneider, R., Huber, K., Weckström, K., 2009. Die Bedeutung des Längssees in Kärnten für die Rekonstruktion der Klima-und Seenentwicklung am Ende der letzten Eiszeit. Innsbruck University Press.

Schmidt, R., Weckström, K., Lauterbach, S., Tessadri, R., Huber, K., 2012. North Atlantic climate impact on early late-glacial climate oscillations in the south-eastern Alps inferred from a multi-proxy lake sediment record. J. Quat. Sci. 27, 40–50. http://dx.doi.org/10.1002/jqs.1505.

Schneider, R., 1978. Pollenanalytische Untersuchungen zur Kenntnis der Spät- und postglazialen Vegetationsgeschichte am Südrand der Alpen zwischen Turin und Varese (Italien). Bot. Jahrb. Syst. 100, 26–109.

Spötl, C., Mangini, A., 2006. U/Th age constraints on the absence of ice in the central Inn Valley (eastern Alps, Austria) during Marine Isotope Stages 5c to 5a. Quat. Res. 66, 167–175. http://dx.doi.org/10.1016/j.yqres.2006.03.002.

Spötl, C., Mangini, A., 2007. Speleothems and paleoglaciers. Earth Planet. Sci. Lett. 254, 323–331. http://dx.doi.org/10.1016/j.epsl.2006.11.041.

Starnberger, R., Rodnight, H., Spötl, C., 2011. Chronology of the last glacial maximum in the salzach palaeoglacier area (eastern Alps). J. Quat. Sci. 26, 502–510. http://dx.doi.org/10.1002/jqs.1477.

van Husen, D., 1987. Die Ostalpen in den Eiszeiten. Verlag der geologischen Bundesanstalt.

van Husen, D., 1997. LGM and late-glacial fluctuations in the Eastern Alps. Quat. Int. 38–39, 109–118. http://dx.doi.org/10.1016/S1040-6182(96)00017-1.

van Husen, D., 2000. Geological processes during the quaternary. Mittl. Österreichischen Geol. Ges. 92, 135–156.

Veit, H., 2002. Die Alpen: Geökologie und Landschaftsentwicklung.

Veselá, P., Lammerer, B., Wetzel, A., Söllner, F., Gerdes, A., 2008. Post-variscan to early alpine sedimentary basins in the tauern window (eastern Alps). In: Tectonic Aspects of the Alpine-dinaride-carpathian System. The Geological Society of London, pp. 83–100.

Vollweiler, N., Scholz, D., Mühlinghaus, C., Mangini, A., Spötl, C., 2006. A precisely dated climate record for the last 9 kyr from three high alpine stalagmites, Spannagel Cave, Austria. Geophys. Res. Lett. 33, 1–5. http://dx.doi.org/10.1029/2006GL027662.

Wirsig, C., Zasadni, J., Ivy-Ochs, S., Christl, M., Kober, F., Schlüchter, C., 2016. A deglaciation model of the Oberhasli, Switzerland. J. Quat. Sci. 31, 46–59. http://dx.doi.org/10.1002/jqs.2831.

Zasadni, J., 2010. Deglaciation of the Zillertal Alps (Austria) in the Lateglacial and Holocene (PhD thesis). Jagiellonian University, Kraków, Poland.

Zasadni, J., 2011. Bericht 2009 über geologische Aufnahmen der quartären Sedimente im Zemmgrund, Schlegeisgrund und im Bereich Dristner und Tuxer Joch auf Blatt 149 Lanersbach, 150 Mayrhofen und 176 Mühlbach. Rep.. Geologische Bundesanstalt, Wien, pp. 138–140.

Zasadni, J., 2014. Bericht 2013 über geologische Aufnahmen von quartären Sedimenten im Zillergrund. Sundergrund und Bodenbach auf Blatt 2230 Mayrhofen. Rep.. Geologische Bundesanstalt, Wien, pp. 327–329.

Zweck, C., Zreda, M., Desilets, D., 2013. Snow shielding factors for cosmogenic nuclide dating inferred from Monte Carlo neutron transport simulations. Earth Planet. Sci. Lett. 379, 64–71. http://dx.doi.org/10.1016/j.epsl.2013.07.023.